



POLITECNICO
MILANO 1863



**“ Steady-state modeling and optimization of
transport refrigeration based on cryogenic fluids
thermal and expansion exergy”**

Academic supervisors from Politecnico di Milano :

Professor Enrico Zio
Professor Luca Molinaroli

Industrial supervisor from Danfoss :

Dr. Ekaterini Krienzi

MSc .Thesis Report

Part 3 of project:

“Optimization of energy/performance in the cooling chain
using cold physical exergy of cryogens”

By :

Vahid Khorshidi

vahid.khorshidi@danfoss.com
vahid.khorshidi@mail.polimi.it

Monday 30th September, 2019

Contents

I	Modeling & Optimization	4
1	Introduction	5
2	Thermodynamic modeling	8
2.1	Thermodynamic states modeling of refrigeration system	8
2.1.1	Cryogen thermodynamic states	9
2.1.2	Vapor compression cycle thermodynamic states	10
2.1.3	HXF thermodynamic states	11
2.1.4	System energy balance equations	12
2.2	Piston expander	13
2.2.1	Intake stroke	13
2.2.2	Power stroke(Expansion stroke)	14
2.2.3	Exhaust stroke	14
2.3	2nd law analysis of the system	15
2.3.1	Heat exchanger	16
2.3.2	Gas pressure drop	16
2.3.3	Liquid pressure drop	16
2.3.4	Expander entropy generation	16
2.3.5	Compressor entropy generation	16
2.3.6	Throttling loss	16
2.4	Components with highest 2nd law losses	17
3	System optimization	17
3.1	Minimizing heat exchanger losses	17
3.2	Optimization on piston expander design parameters	18
3.3	Improvements on cryogenic heat exchanger(Various cryogen)	22
3.4	Modifications on vapor compression cycle	23
3.4.1	Various refrigerant	23
3.4.2	VCC component modifications	23
3.5	Two-stage expansion	25
4	Off-design conditions and system performance variations	26
4.1	Ambient temperature	26
4.2	Evaporator temperature	27
4.3	Cooling power required	27
5	Conclusion	28

Disclaimer

The contents of this report is based on the the information in the reference section and assumptions that made where it has been relevant. The initial title of the project "Optimization of energy/performance in the cooling chain in combination with the Dearman approach" was changed to "Optimization of energy/performance in the cooling chain using cold physical exergy of cryogenes" to encompass a wider range of alternative solutions for comparison. Based on the information by Dearman co. and the preliminary study performed, it has been decided to focus on the transport application of Dearman engine considering the fact that it is the most viable application.

Part I

Modeling & Optimization

Abstract

This work of research is focused on the steady-state modeling and optimization of transport refrigeration using combined cooling and expansion work of cryogenic fluids. The proposed refrigeration system consist of three main flows: cryogenic fluid, refrigerant and heat exchange fluid. These 3 flows exchange heat and work within one integrated system that provides cooling effect to the cooling compartment. The main system components are cryogenic heat exchanger, cryogenic piston expander and a conventional vapor compression cycle(VCC). Mass and energy equations are solved together directly to find the thermodynamic states of the system. The 2nd law of thermodynamics analysis has been adopted to spot the irreversibilities distribution that leads to decent understanding of components with the most entropy generations for further improvements on the system. This analysis been performed for various cryogens: liquefied nitrogen(LiN), Liquefied air(LiA), Liquefied natural gas(LNG) and liquefied hydrogen(LiH); according to results, 2 latter are capable of producing 11 kw and 12 kw of cooling from physical exergy while chemical exergy is consumed to provide power-train. Based on the distribution of entropy generations, cryogenic HX, expander exhaust and compressor in VCC are the largest losses in the system. For the expander design, optimization algorithms were used while satisfying certain mechanical, structural and system constraints. Moreover, the effect of different refrigerants and various system component levels is examined. Finally the off-design condition is considered under 3 varying conditions: ambient temperature, required evaporator temperature and cooling load required.

Nomenclature

ΔP	Pressure drop or difference(bar)	PM	Particulate matter
ΔT_{min}	Minimum temperature difference achieved in a heat exchanger flows	$Q_{C\ in\ Exp}$	Heat absorbed by cryogen inside the expander (W)
\dot{m}	Mass flow rate (Kg/s)	$Q_{Cond\ R}$	Heat absorbed by cryogen inside the expander (W)
η	Efficiency of a process(-)	$Q_{HX\ in\ Exp}$	Heat absorbed by HXF inside the expander (W)
η_{Aux}	Efficiency due to auxiliary power consumption	R_s	Shaft radius (m)
η_{Shaft}	Efficiency of the shaft between compressor and expander	R_U	Universal gas constant ($\frac{J}{K.Mol}$)
ρ	Density(kg/m^3)	RPM	Revolution per minute(60/s)
θ	Angle between crankshaft and shaft pin center line(degree)	T	Temperature (K)
c	Speed of light in a vacuum inertial frame	VCC	Vapor compression cycle
D_{bore}	Bore diameter of piston(m)	W_{Comp}	Work supplied to the compressor (W)
f	Frequency of piston expander (1/s)	W_{Exp}	Work produced in the expander (W)
GWP	Global warming potential(Relative to CO_2)	Z	Compressibility factor(-)
HXF	Heat exchange fluid	Z_P	Distance of piston from top dead(m)
L_r	Length of connecting rod (m)	Subscripts	
l_{dv}	Dead volume length of piston(m)	amb	Ambient condition at 293.15(K) and 101325 (Pa)
LiA	Liquefied air	Aux	Auxiliary power consumption
LiH	Liquefied hydrogen	C	Cryogenic fluid(cryogen)
LiN	Liquefied nitrogen	exp	Cryogenic flow expander
LNG	Liquefied natural gas	HX	Heat exchange fluid
MM	Molecular mass(g/mole)	in	Components inlet side
ODP	Ozone depletion potential(Relative to CFC 11)	$Isen$	Isentropic process
P	Pressure(Pa)	out	Components outlet side
		R	VCC refrigerant
		$Shaft$	Shaft between compressor and expander
		x	This is a superscript

1 Introduction

Refrigeration is one of the challenges of the new world; As a growing sector and as an inevitable corollary of rising population and global warming. It is expected that cooling energy demand surpass the energy needed for heating by 2060. Furthermore, it is projected a 6-fold increase in number of refrigerated vehicles. The predicted fleet size if 1.2 million TRUs in Europe in 2025 estimated to produce 39 million ton of CO_2 , 120 000 ton of NO_x and 15000 ton of PM per year.

The current fleet based on data from Cemafruid co. is estimated to be 1 million unit mostly running on diesel, to make situation even worse, they are using secondary diesel engine which produces 14 times more particulate matter(PM) and 6 times more NO_x than primary diesel engine used for power-train.[3] Current refrigerated vehicles rely heavily on fossil fuel and mainly on diesel, lead to high level of toxic pollutants specially in urban areas. This study revolves around this application; evaluating the possibility of a shift from diesel based cooling to a more sustainable way. Expansion and cold exergy extraction engine as a cutting-edge technology can redress this need in form of a sustainable low- CO_2 cooling system with lower impact on Ozone layer compared to conventional technology. It is worth mentioning that cryogenic fluid used for example, liquefied nitrogen (LiN), can be easily produced by pressurizing air which only needs electricity. This electricity can be provided at off-peak hours of consumption from renewable sources that can be used as a storage method of intermittent renewable energy.[2, 3]

A comparison of competitive sustainable technologies for future of transportation is available in literature as Lin [33] who performed software simulation on the alternative fuels energy use and emissions. Another Well-to-Wheel analysis has been performed by US energy department[34] which takes a comprehensive look on the all possible scenarios based on fuel-cycle model. In

Table 1: Assumed values and parameters in the simulation

Parameter(unit)	Value
Temperature(k)	
Refrence condition(ambient)	298.15
Evaporator design point	243.15
Sub-cooling	-4
Superheating	5
Minimum temperature difference(k)	
Water-cooled HX	3
Air-cooled HX	6
Pressure(Pa)	
Refrence condition(ambient)	101325
Mechanical limit of piston expander	5e+6
Pressure drops percentage(%)	
Suction of compressors	1
Discharge of compressors	1
Evaporator	5
Condenser	2
Efficiencies(%)	
Electro-mechanical	97
Pumps	90
Isentropic of compressors	65
Isothermal piston expander	65
Discharge coefficient of inlet/outlet valves of expander	0.75
Auxiliary consumption as percent of work produced(%)	10
Methane molar ratio in LNG(%)	100

another study by European commission, the Well-to-Wheel analysis on alternative fuel has been performed indicating the cheapest fuels in Europe in price per 100km in euros are: 4.24, 4.27, 5.678, 5.678 for electricity, fuel cells, Bio-gas and natural gas respectively.[37] Regarding the transport refrigeration there are not many resources available, considering this, an overview study has been performed and the list of possible scenarios has been narrowed down to: Internal combustion engine based on CNG(or LNG), fully electric with Li-Ion batteries , fuel cell powered refrigeration and combined physical exergy and expansion work using various cryogens. The summary of the comparisons indicated on table 2. It is assumed that the TRU is used on average 12 hours a day; 6 hours on the road(cooling requirement of 15 kw) and 6 hours parked with cooling requirement of 5 kw. For the cases of "LNG as cryogen" and "LiH as cryogen" the price is calculated based on extra components required (ICE and PEM FC respectively) for 6 hours the truck is parked and the container needs to be self sustained in terms of cooling as there is no possibility of getting cold exergy from truck fuel. [3]

The results of initial comparisons showed unrivalled cost per KWh(€/KWh) of cooling by combined cool and power of engine running on LNG(to extract physical exergy of fluid) and hydrogen(for pressure exergy extraction). Considering the potentials, cryogenic expansion and cooling, was selected to be developed further with help of modeling and simulations tools. Dorosz et al performed exergetic analysis on cold exergy utilization in transportation focusing on the thermal exergy of the fluid, showing the cooling produced can be as high as 7 kw(based on fuel consumption of a truck equal to 20 Kg/h). It is also considered the possibility of direct expansion work of LNG at 283K.[26]

Nitrogen as an easy to produce candidate cryogen is mostly produced by means of "Cryogenic distillation" of air; Currently there are plants working on liquid air storage systems with AC to AC electricity round trip efficiency of stand alone systems around 60% [2] this indicates the potentials of LiN usage as a energy carrier.

In the literature there are several applications of cryogenic fluids cold exergy, here we consider only cases involving both cooling potential from latent and sensible heat and expansion work.(Physical exergy = Thermal exergy + Pressure exergy) Szczygiel[23] analysed the exergy conversion of LNG to electricity for regasification in LNG terminals. Gomez et. al [24] evaluated various technologies based on the heat source available. Narrowing it down to our area of interest

Table 2: Well-to-Wheel analysis of various sources for refrigerated vehicle

Fuel type	Cost of ownership in 10 year (Cooling only) [€/TRU]	Ton CO2 equivalent in 10 year [TCO2/ 10 year/TRU]
Diesel	270k	325
CNG	170k	215
Electricity	130k	235
hydrogen	240k	300
nitrogen as cryogen	238k	300
LNG as cryogen	120k	60
hydrogen as cryogen	120k	42

is a standalone system for transport refrigeration. There is a patent on LNG pressure and thermal exergy for air-conditioning for LNG cars [25],

A study by Tianbiao et al. took a look at the exergy losses in wasted energy of LNG; various scenarios were proposed: a closed loop organic Rankine cycle and a turbine to extract heat from pressurized natural gas, An air separation unit using only the thermal exergy, freeze desalination, cryogenic CO_2 capture, Use of secondary fluid for data centers cooling and LiA or LiN production for later consumption as power production. [40]

Inkyu et. al proposed a novel approach to utilize the cold exergy of LNG in combination with liquid air storage. Use of cold exergy in this configuration leaded to 11.04% of energy saving compared to the base case. Yajun et al also performed similar study showing the 38% gains compared to the usual process when the cold exergies of LNG is used. [36, 38] The abundant cold exergy potential in regasification plants can bring the price of LiA or LiN low enough to make cooling based on cryogenics competitive to current technologies specially for transport refrigeration that is dominated with direct diesel driven VCCs.[3]

Dearman Engine Company Ltd has launched prototype of similar systems running on liquefied nitrogen as cryogen that consist of a LiN Cryogenic tank, a piston expander and a refrigeration cycle as shown in fig. 1. The cooling process starts with flow of LiN form cryogenic vessel(at $P = 2$ bar)in the cylinder of the engine; coming into contact with heat removed from inside refrigerated container that causes vaporization and expansion of the LiN lead to work extraction from the piston as shown in fig.9. Finally, this expansion work powers a refrigeration cycle and auxiliaries (fans, pumps and etc.). Cooling from refrigeration cycle accounts for nearly half of total heat absorbed from container.[35] This system increases efficiency by 50% compared to conventional systems that are using LiN thermal exergy and reduces time for cooling a vehicle from $+15^{\circ}C$ to $-21^{\circ}C$ to less than 30 minutes. [3]

Another study by Jia et al. proposed a combined open-closed cycle capable of utilizing up to 39% of expansion exergy of LiA. This includes a conventional expansion engine with a closed loop Stirling engine to maximize the work output of the system.[39]

Hydrogen on the other hand has huge amount of physical exergy in the form stored as in fuel cells vehicles container. The common form of storage is pressurized hydrogen at 350 to 700 bar; this means there is high pressure exergy that can be extracted from the flow before dropping the pressure to 2 bars for using in fuel cell. Valenti [19] proposed a highly efficient liquefaction process of hydrogen which can reach 2nd law efficiency of 48% with hydrogen entering as 60 bar of pressure. This can increase the energy density and range of hydrogen fuel cell and can double the amount of cooling per kg since the thermal exergy can also be extracted. Transition in the road transport industry towards PEM fuel cells is becoming more probable due to high energy density of hydrogen, possibility of having long range and causing no pollution (on the pump-to-wheel phase).

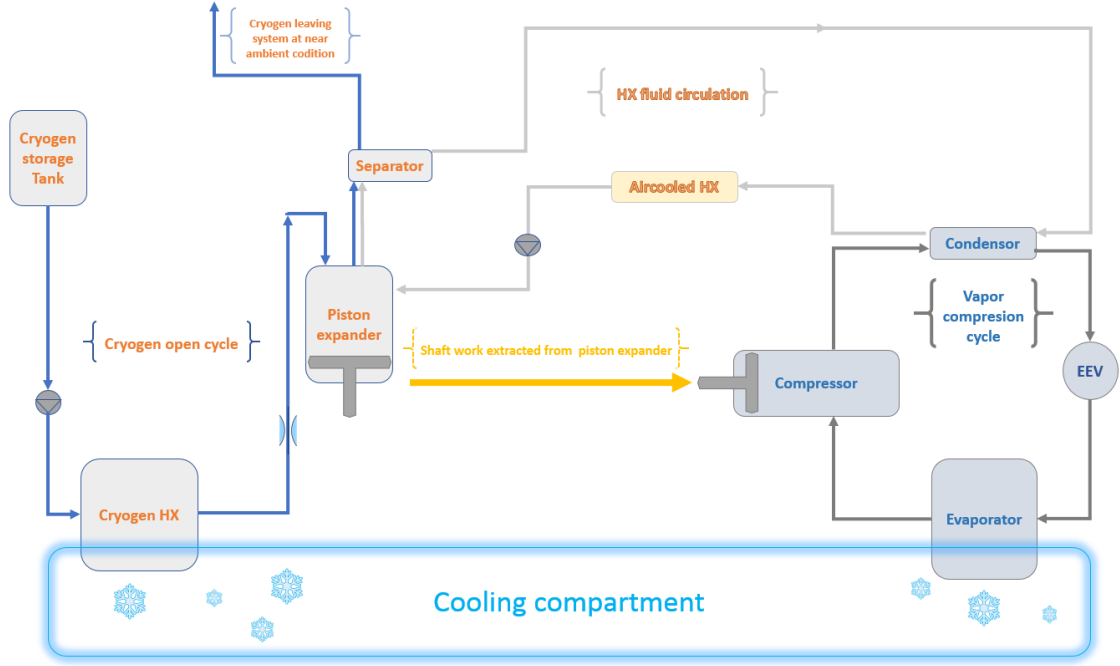


Figure 1: Combined refrigeration system using cryogenic expander engine

LNG and hydrogen as cryogen means the cooling depends on power-train; in fig.2 the simplified schematic of the system is shown.

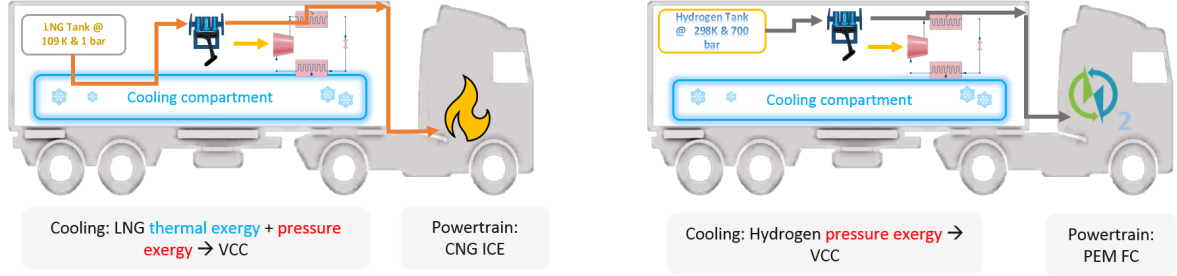


Figure 2: Combined refrigeration and power-train system using cryogenic expander engine, Liquid fuel system(on the left) and compressed gas system(on the right)

2 Thermodynamic modeling

2.1 Thermodynamic states modeling of refrigeration system

There is a wide range of studies dedicated to VCC simulations and modeling, among which the steady-states approaches are relevant to this study. In this regards there are various softwares developed for steady-state simulations of VCCs. VapCyc by D.Richarson [5] is one of the tools initially considered, though due to limitations on system modifications and lack of an integrated solution for the whole system has been ruled out. EES is considered as a robust way of solving thermodynamic states equations; the main obstacle on using EES is in the nature of the modeling that holds some uncertainties in equation requiring iterations and requirements of optimization methods. The key feature that separates this from other conventional VCC problems lies in the 3 main flows interacting with each other: Cryogenic expander-heat exchanger line, VCC and heat exchanger line. Considering the challenges it was decided to build our objected oriented program in Python environment based on properties from CoolProp. [6] The main class created represents the thermodynamic states while there are sub-classes representing the states of each fluid within the system. Energy(1st law of thermodynamics) and mass balances were used to find the next

state based on the one before. Functions were defined as well to apply each component's effect on the states; compressors, heat exchanges, pressure drops and efficiency's.

2.1.1 Cryogen thermodynamic states

Starting from storage tank at near ambient pressure and temperature just below its normal boiling temperature of cryogen. Cryogen flow then exchanges heat with cooling compartment at this point the temperature reaches close to the the cooling compartment temperature ($\Delta T = \Delta T_{min}$ lower), then the super-critical flow of cryogen throttled to pressure in the range suitable for expander operating condition. The fundamentals of the cryogen line is depicted in fig. 3.

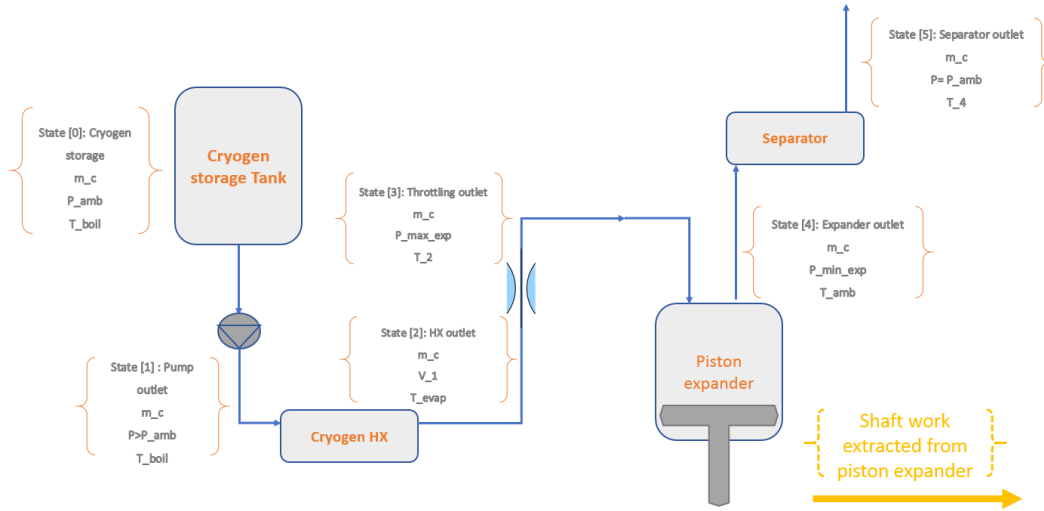


Figure 3: Cryogen path in the refrigeration system, from storage tank to ambient.

For liquid hydrogen, the process is the same with the only difference that the boiling temperature is lower (20K). The mass flow rate out of tank that is controlled to keep the temperature at certain set point based on the cargo requirements. Then it exchanges heat in a cryogenic heat exchanger. The next step is to exchange heat with warm HXF coming out of condenser. Up until this point only thermal exergy is exploited. Finally the pressure exergy is extracted in the expander when cryogen undergoes near isothermal expansion. In case of compressed hydrogen there is only HXF fluid heat exchange and the pressure exergy that can be used. P-H and T-S diagrams with states of each step is indicated in fig. 4 and 5 respectively.

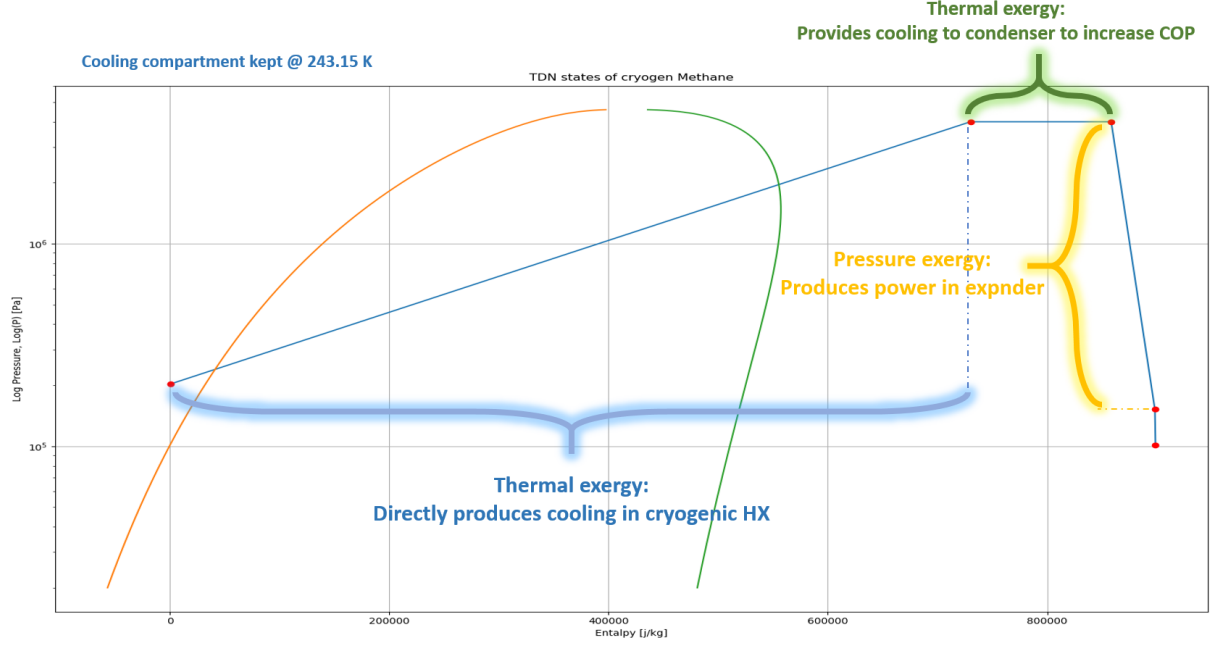


Figure 4: P-H diagram of LNG and exergies that can be exploited.

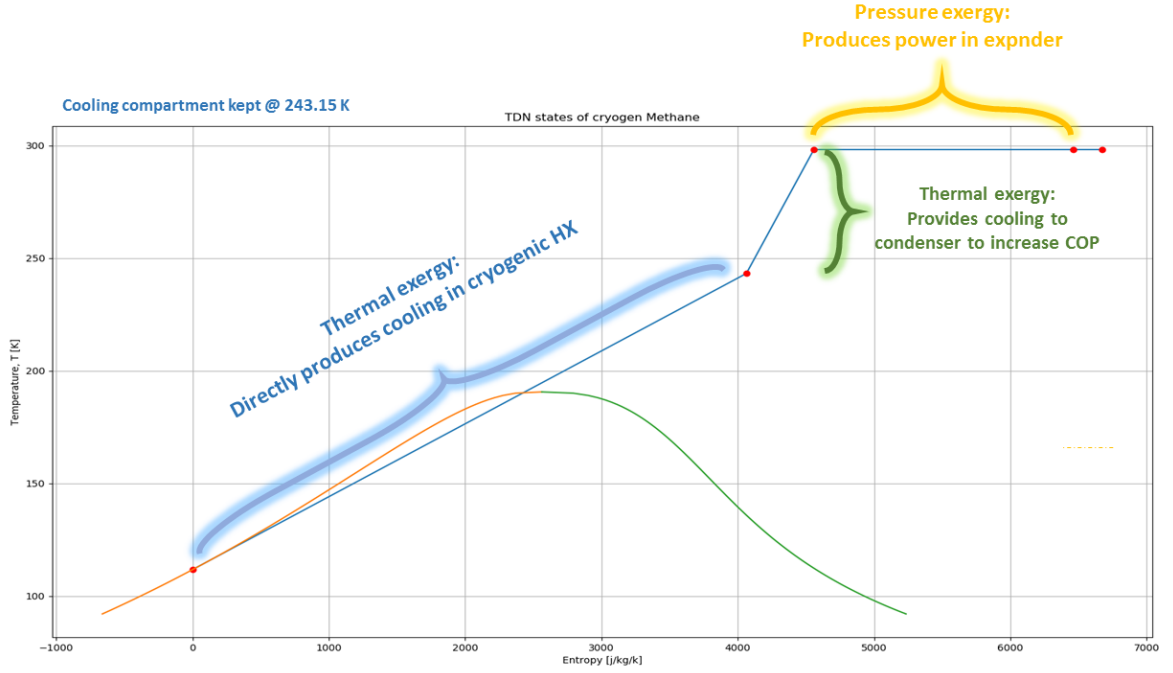


Figure 5: T-S diagram of LNG and exergies that can be exploited.

2.1.2 Vapor compression cycle thermodynamic states

For the VCC the evaporator thermodynamic(TDN) state is calculated based on temperatures of evaporator and condenser that is already fixed. A simplified schematic of 4 component VCC is displayed in fig. 6. For implementation in code the number of points is calculated as follows:

$$\# \text{ of TDN states} = \# \text{ of components} + \underbrace{\# \text{ of } \Delta P}_{\text{Pressure drops}} + \underbrace{\# \text{ of } \Delta T}_{\text{Temperature variations}} + \underbrace{1}_{\text{To close the cycle}} \quad (1)$$

Pressure drops : evaporator(phase change to vapor causes drop in pressure), condenser, suction and discharge side of compressor, liquid line losses.

Temperature variation: sub-cooling and super-heating.

- Compressor: The compressor outlet enthalpy can be calculated based on isentropic efficiency:

$$h_{out} = h_{in}(h_{isen} - h_{in})\eta_{isen} \quad (2)$$

where h_{in} and h_{isen} are the inlet and isentropic enthalpy and η_{isen} is the isentropic efficiency that is function of pressure ratios, compressor type and rotational velocity [20]:

$$\eta_{isen} = c0 + c1N + c2N^2 + c3\left(\frac{p_{out}}{p_{in}}\right) + c4\left(\frac{p_{out}}{p_{in}}\right)^2 \quad (3)$$

Where N is the rotational velocity(RPM) and constants are based on laboratory measurements of the manufacturer.

- Electric expansion valve(EEV): The process occurring in the EEV is considered to be isenthalpic ($h_{in} = h_{out}$) and the pressure drop can also be calculated by:

$$\Delta P = \frac{\dot{m}^2}{(K_v A_e)^2 \rho_{in}} \quad (4)$$

Where K_v is the expansion coefficient and A_e is the ratio of expansion valve area available for flow to pass through.

- Receiver: Considering that the system is assumed to be working in steady state so it is expected that the flow entering and exiting have same quality of vapor:

$$\dot{m}_i = \dot{m}_o^{liquid} + \dot{m}_o^{vapor} \Rightarrow \begin{cases} \dot{m}_o^{liquid} = \dot{m}_i(1 - Q_i) \\ \dot{m}_o^{vapor} = \dot{m}_i Q_i \end{cases} \quad (5)$$

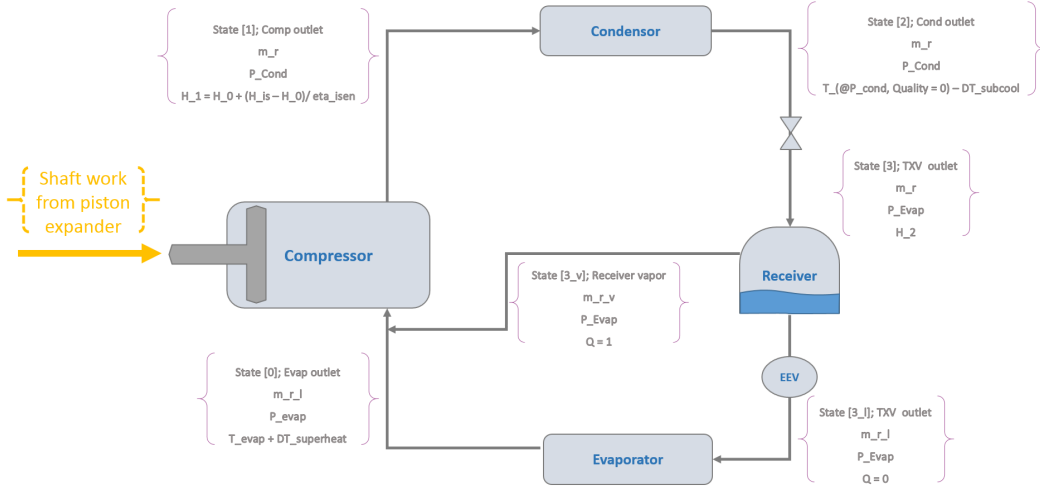


Figure 6: Simplified refrigerant path in the vapor compression cycle.

2.1.3 HXF thermodynamic states

Heat exchange fluid used in the modeling is Ethylene Glycol 60% (CoolProp mixture Water/ASHRAE)[6] with water. As shown in fig. 7 the fluid passes through 5 components. Starting from separator at near ambient condition(state 0) moving to the condenser(state 1) where it absorbs the heat and then releases a portion of the heat at air-cooled HX denoted as Q_{out} (state 2) before being pumped to the expander. In the expander the HXF ensures near isothermal process(state 3) and finally the exhaust is sent to separator(state 4).

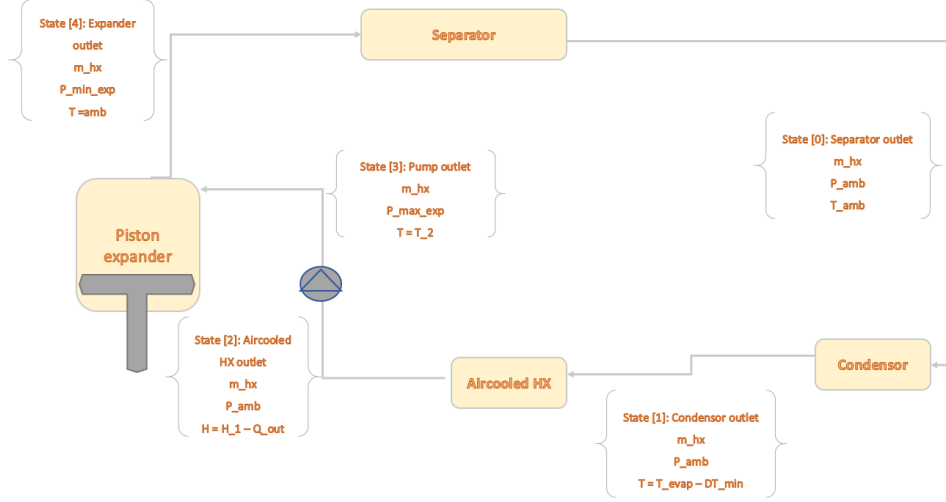


Figure 7: HXF path cycle, from condenser to separator.

2.1.4 System energy balance equations

Once the states are known it is possible to find the mass flow rate for each flow line (M_{dot}); Energy balances on expander, condenser and compressor work respectively gives :

$$\begin{bmatrix} W_{Exp} + Q_{C \text{ in } Exp} & 0 & -Q_{HX \text{ in } Exp} \\ 0 & Q_{Cond \text{ R}} & -Q_{HX \text{ in } Exp} \\ W_{Exp} * \eta_{Shaft} * \eta_{Aux} & -W_{Comp} & 0 \end{bmatrix} * \begin{bmatrix} M_{dot}^C \\ M_{dot}^R \\ M_{dot}^{HX} \end{bmatrix} = \begin{bmatrix} 0 \\ Q_{Air-cool} \\ 0 \end{bmatrix} \quad (6)$$

This equation is solved iteratively considering that $Q_{Air-cool}$ is also unknown, the constraint is that the system should achieve 15 KW of cooling as total cooling effect in the cooling compartment and it should provide enough heat in the expander to keep it near isothermal process at near ambient temperature. in fig.8 the mass flow rate required to produce 15kw of cooling and the corresponding HXF and refrigerant needed can be observed.

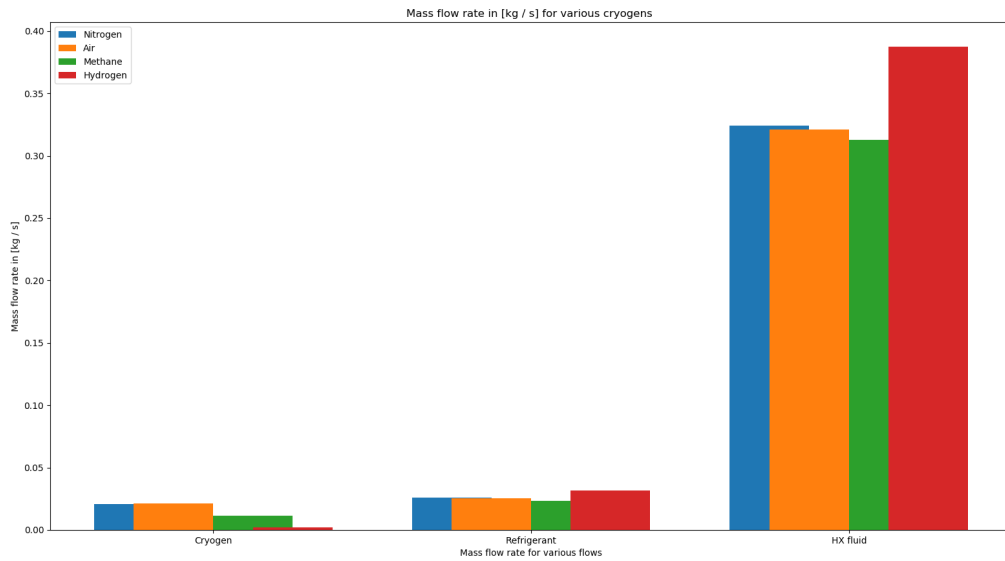


Figure 8: Mass flow rates of various cryogen with the corresponding HXF and refrigerant mass flow rate.

2.2 Piston expander

As indicated in fig. 9, the single piston expander has 3 strokes; at intake stroke's initial degrees, warm HXF(Ethylene Glycol 60%) that absorbed heat from condenser is pumped into the chamber. At top dead center this valve is closed and the cryogen valve opens allowing high pressure cryogen to enter the piston expander. As soon as the cryogen valve closes, the near isothermal expansion is initiated(power stroke). When reaching bottom dead center, the exhaust valve is switched open that let the nitrogen and HXF move to the separator.

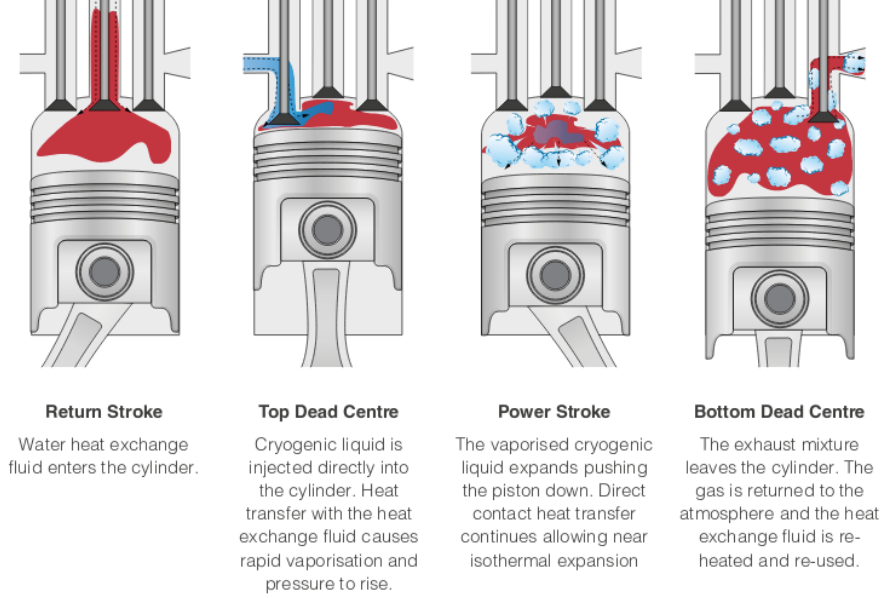


Figure 9: Dearman piston expander various states

The piston expander consist of a cylinder with 3 valves(cryogen, HXF and exhaust), piston sliding in the cylinder which is connected with connecting rod to crank that transfers power to crankshaft. As indicated in fig. 10, the engine is three stroke with HX valve opening before top dead center position and cryogen valve opening right at top dead center(HX valve is shut at this point). Power stroke occurs right after and continues till bottom dead center [14, 15, 16].

$$Z_P = r_s(1 - \cos(\theta)) + L_r \left(1 - \sqrt{1 - \left(\frac{r_s}{L_r}\right)^2 \sin^2 \theta} \right) \quad (7)$$

$$V_C = (Z_P + L_{dv}) \frac{\pi D_{bore}^2}{4} \quad (8)$$

There are several design parameters defining an expander, each affecting the system performance.

As indicated in fig. 10, D_{bore} is the bore diameter, L_{dv} is the dead volume length, Z_P is the distance piston has from dead top position, L_r is the length of connecting rod and θ represents the angle defining the state and piston position. Cryogen valve opening degree is inversely correlated with the maximum work output.

2.2.1 Intake stroke

Due to high pressure difference at the intake, it should be checked for the choking condition:[8]

$$P_{choke} = P_{in} \left(\frac{2}{\gamma + 1} \right)^{\frac{\gamma}{\gamma - 1}} \quad (9)$$

In case $P_{expander} < P_{choke}$:[8]

$$\dot{m}_{in} = C_d A \sqrt{\gamma \rho_0 P_0 \left(\frac{2}{\gamma + 1} \right)^{\left(\frac{\gamma+1}{\gamma-1}\right)}} \quad (10)$$

Where, C_d is the discharge coefficient, $A = \frac{\pi D_{valve}^2}{4}$ is the inlet area, $D_{valve} = \frac{D_{bore}}{ratio_{B/V}}$, γ is the heat capacity ratio($\frac{C_p}{C_v}$), ρ_0 is the density of fluid at the inlet and P_0 is the pressure of the flow at the inlet. It should be noted that \dot{m}_{in} unit is $\frac{mass}{second}$ but the intake occurs only in $\frac{\theta_{CC}}{360}$ that means the calculated \dot{m}_{in} should be divided by the aforementioned ratio to get the \dot{m}_{in}^{Real} .

And the pressure drop is calculated assuming valves opening acting as an orifice [9]:

$$\Delta P = \frac{1}{2} \rho (1 - ratio_{B/V}^4) \left(\frac{Q}{C_d A_o Y} \right)^2 \quad (11)$$

While, Q is the volume flow rate, C_d the discharge coefficient, A_o the orifice opening area and Y is the expansion factor(1 for incompressible flow). Y is estimated for compressible flow using ISO 5167-2, accordingly:

$$Y = 1 - (0.351 + 0.256(1/ratio_{B/V})^4 + 0.93(1/ratio_{B/V})^8) \left(1 - \left(\frac{P_{s,2}}{P_{s,1}} \right)^{1/\gamma} \right) \quad (12)$$

To check if the flow is considered compressible it is required to compare its velocity at valve exit with Mach number[8]:

$$M = \left[\left(\frac{p_{in}}{p_{out}} \right)^{\frac{\gamma-1}{\gamma}} \frac{2}{\gamma-1} \right]^{\frac{1}{2}} \quad (13)$$

In case velocity in the exit of valve is larger than $0.3M$ the flow is compressible and Y should be calculated as in eq. 12.

2.2.2 Power stroke(Expansion stroke)

Moving from cryogen valve closed (state 1) to dead bottom center (state 2) is the power production stroke, the former is denoted as Z_{CC} (Cryogen valve closed) and the latter with Z_{EO} (Exhaust valve opened) corresponding to θ_{CC} and θ_{EO} (assumed 180°) respectively. From ideal gas law we have :

$$W_{Isothermal} = P_{in} V_{EO} \ln \left(\frac{V_{CC}}{V_{EO}} \right) \quad (14)$$

Considering the desired pressure ranges(40 bar and bellow), the compressibility factor values of cryogens (except for Methane) are very close to 1, it can be assumed the $W_{Isothermal}$ can be calculated with the ideal gas assumption. The work output improvements can also be verified using the enthalpy and entropy changes of initial and final states:

$$(\Delta U)_T = U_2 - U_1 \quad (\Delta S)_T = S_2 - S_1 \longrightarrow Q_T = T \Delta S_T \quad (\Delta U)_T = Q_T + W_{Isothermal}^{Real} \quad (15)$$

Simplified to :

$$W_{Isothermal}^{Real} = (\Delta U)_T - T \Delta S_T \quad (16)$$

2.2.3 Exhaust stroke

Same procedure as in intake stroke can be repeated here using eq. 10, which provides the suitable valve opening diameter, and then eq. 11 can be used to calculate pressure drops.

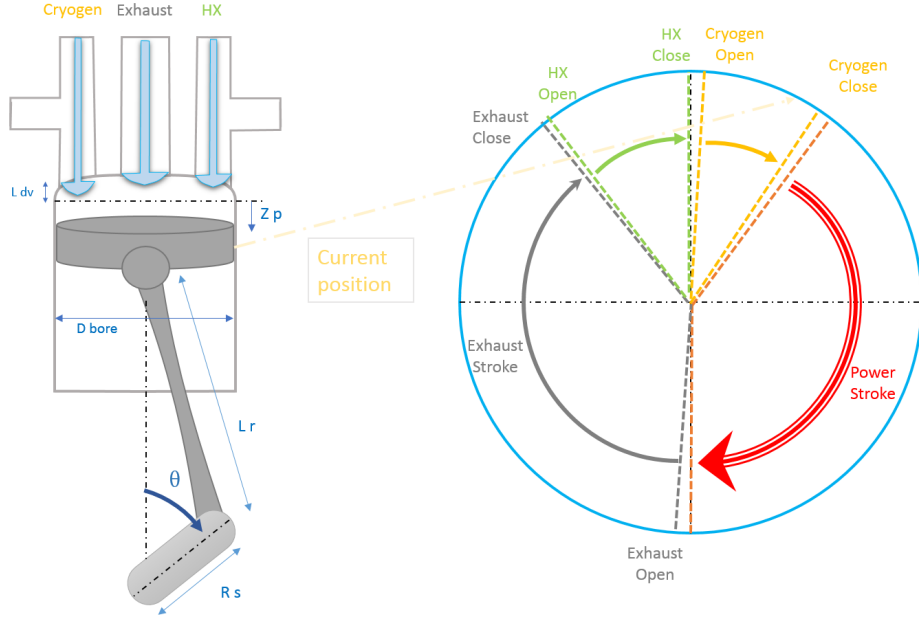


Figure 10: Piston expander parameters(on the left) and θ variations with the time and its implications (on the right) .

The P-V diagram of cryogen expansion in initial design of piston expander is depicted in fig. 11, it should be noted that the pressure drop during exhaust and losses due to high frequencies are neglected.

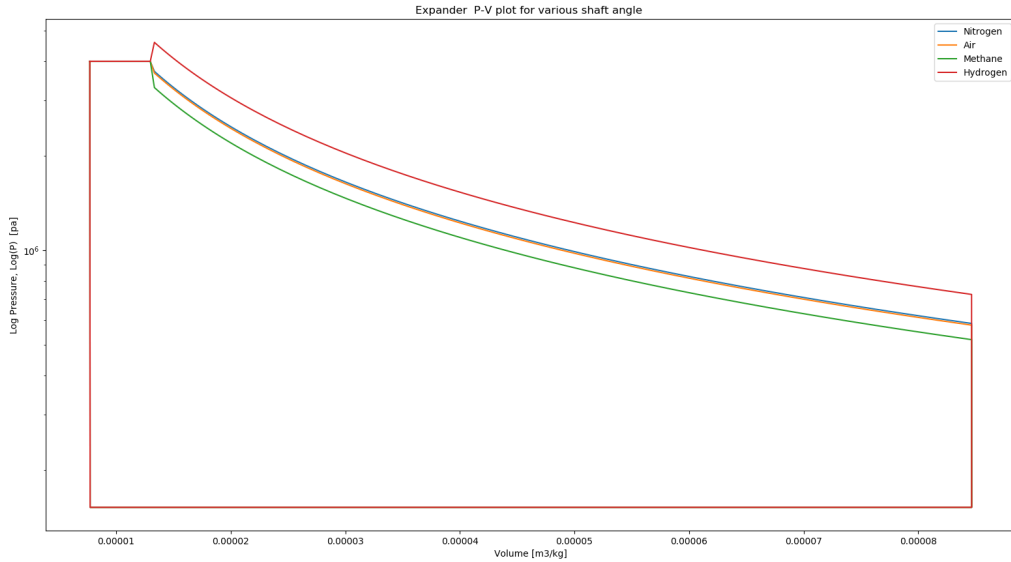


Figure 11: Expander ideal P-V plot of 4 selected cryogenes for initial guess design values.

2.3 2nd law analysis of the system

2nd law of thermodynamics enables the possibility of identifying the main sources of energy losses, also processes and parameters to modify in order to enhance the performance of the system. Starting from reversible system while deducting the sum of works lost due to irreversibility. Exergy analysis has an edge over other methods in term of inherent capability of including all stream properties (Temperature, pressure and composition). The main goal is to calculate the irreversibility distribution and spot the critical components to minimize losses with proper system modifications.

The entropy generations were calculated for 3 flow lines based on the equations provided in each section.

2.3.1 Heat exchanger

There are several heat exchangers in the system, they are divided into two main categories: flow exchanging heat with an environment with constant temperature and the other type is two flows exchanging heat with constant heat capacity(generic formula). For the generic case:

$$dS = \frac{dQ}{T} \text{ \& } \Delta S_{HX} = \Delta S_{cold \text{ flow}} + \Delta S_{hot \text{ flow}} = \int_{out}^{in} \frac{dQ_{cold}}{T} + \int_{out}^{in} \frac{dQ_{hot}}{T} \quad (17)$$

Considering equal amount of heat exchanged between hot and cold sides :

$$\Delta S_{HX} = Q \left(\frac{\ln\left(\frac{T_{cold}^{in}}{T_{cold}^{out}}\right)}{T_{cold}^{in} - T_{cold}^{out}} - \frac{\ln\left(\frac{T_{hot}^{out}}{T_{hot}^{in}}\right)}{T_{hot}^{out} - T_{hot}^{in}} \right) \quad (18)$$

2.3.2 Gas pressure drop

For the pressure drops of gas phase:

$$\Delta S_{Gas\Delta P} = \dot{m} \frac{R_U}{MM} \int_{P_{out}}^{P_{in}} \frac{ZT}{P} \frac{dP}{T} \quad (19)$$

After integration becomes:

$$\Delta S_{Gas\Delta P} = \dot{m} \frac{R_U}{MM} \bar{Z} \ln \left(1 + \frac{\Delta P}{P_{Out}} \right) \quad (20)$$

2.3.3 Liquid pressure drop

Similarly can be shown that:

$$\Delta S_{Liquid\Delta P} = \dot{m} V \frac{\Delta P}{T} \quad (21)$$

2.3.4 Expander entropy generation

For the expander it is possible to start from the ideal work that can be extracted from a flow,

Accordingly:

$$\begin{aligned} \eta_y &= \frac{dW_{real}}{dW_{ideal}} \quad V = Z \frac{R_U}{MM} \frac{T}{P} \\ dW_{Wasted} &= TdS = dW_{real}(1 - \eta_y) = -mvdP(1 - \eta_y) \\ \Delta S_{Expander} &= \int_{P_{out}}^{P_{in}} \frac{ZT}{P} \frac{\dot{m}(1 - \eta_y)}{T} dP = \frac{\dot{m}R_U}{MM} \bar{Z}(1 - \eta_y) \ln \left(\frac{P_{in}}{P_{out}} \right) \end{aligned} \quad (22)$$

2.3.5 Compressor entropy generation

The derivation is very similar to that of the expander:

$$\Delta S_{Compressor} = \frac{\dot{m}R_U}{MM} \bar{Z} \frac{(1 - \eta_y)\bar{\eta}_y}{l} n \left(\frac{P_{out}}{P_{in}} \right) \quad (23)$$

2.3.6 Throttling loss

Throttling loss can be calculated based on the stagnation properties of a flow . The entropy generation for this process is calculated by:

$$\Delta S_{Throttling \text{ loss}} = -\dot{m} \frac{R_U}{MM} \ln \left(\frac{P_t^{out}}{P_t^{in}} \right) \quad (24)$$

Where P_t^{out} and P_t^{in} are pressure values at stagnation enthalpy in the outlet and inlet respectively.[7]

2.4 Components with highest 2nd law losses

Results of the 2nd law analysis on the the whole system indicated the components with major entropy generations, the 6 most contributing components are depicted in fig.12.

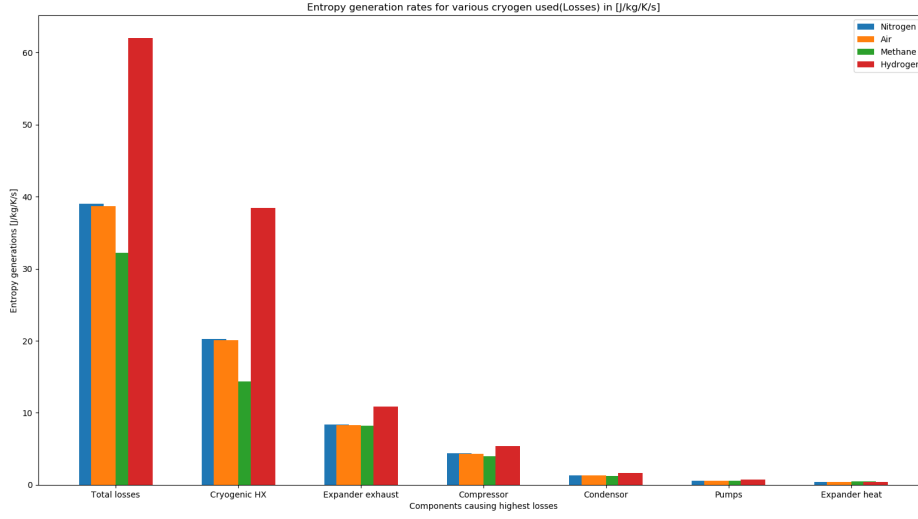


Figure 12: Total losses and 6 components with most entropy generations

3 components are responsible for 85% of losses, in order of magnitude they are: Cryogenic heat exchanger, expander exhaust and compressor.

In fig.13 the entropy generations are depicted as well as the initial efficiency for a system of LiN.

3 main component were selected in order to perform the optimization on.

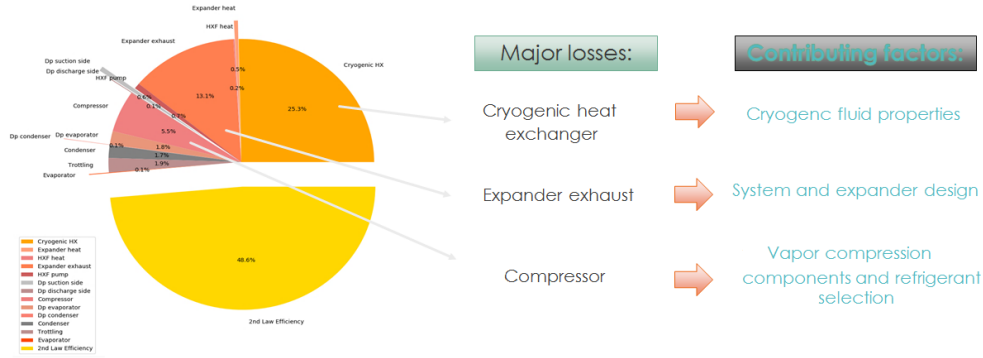


Figure 13: Distribution of entropy generation for various components and major losses with the main component or system responsible for

The biggest loss is related to the cryogenic HX; this loss depends on the inlet temperatures and the amount of heat exchanged. The 2nd most entropy generation is due to the expander design; leading to the need for improvements on this component in order to minimize the piston expander exhaust; this task can be done with specifically designing the expander for each cryogen as well as optimum selection of design parameters. The 3rd largest loss is in compressor, this means improvements on VCC and to be specific, on compressor will decrease this loss.

3 System optimization

3.1 Minimizing heat exchanger losses

The cryogenic HX loss depends on the inlet temperatures of hot and cold flow and the magnitude of the heat transferred. Considering the fixed reefer temperature, the only remaining parameter

would be the normal boiling temperature of the cryogen which is only fluid dependant and as shown in fig. 14 there is a direct correlation between the normal boiling temperature and the 2nd law efficiency. Storage condition of cryogen also plays important role, the cryogenes can be kept at higher pressure and higher temperatures in the storage tank to increase the 2nd law efficiency and increases the round-trip efficiency by decreasing the liquefaction energy requirement. On the down side the amount of cooling per kg of cryogen diminishes as the thermal exergy quantity decreases.

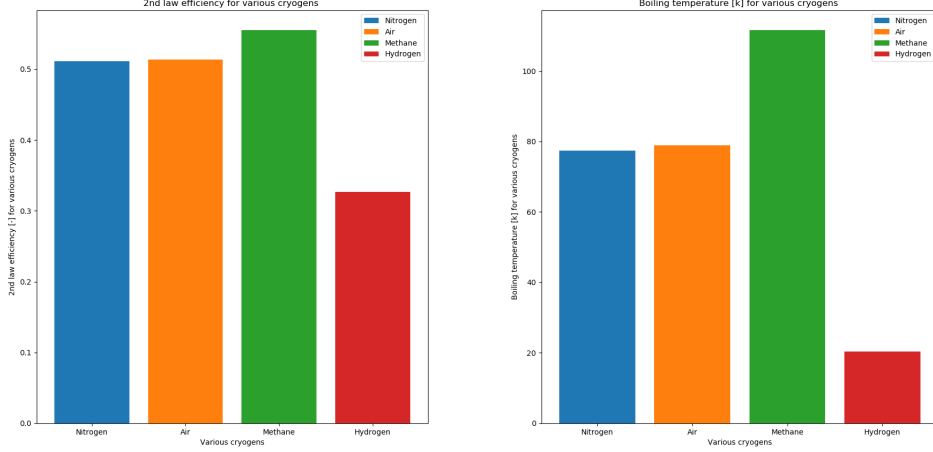


Figure 14: Boiling point of cryogen and 2nd law efficiency comparison.

3.2 Optimization on piston expander design parameters

There can be two approaches for optimizing for power output of expander:

- Ideal gas model
- Real gas model

First method would give a general understanding of the system given that the objective function depend only on initial and final condition pressure ratios and it is not correlated with absolute pressure values. Accordingly, the model simplifies to maximizing minimum and maximum volume ratios in piston expander. While in real gas model, the aim is to maximize the work by finding the thermodynamic states that release the highest amount of work, which is dependant on absolute values of pressure. The main goal of optimization here is to maximize the work output while satisfying certain constraints. As shown in eq. 14 the work based on ideal gas assumption can be maximized when the ratio of $\frac{V_{CC}}{V_{EO}}$ is maximized. in other words:

Objective function:

$$Max \left[(r_s - r_s \cos(\theta_{CC}) + L_r (1 - \sqrt{1 - (\frac{r_s}{L_r})^2 \sin^2 \theta_{CC}}) + L_{dv}) \frac{\pi D_{bore}^2}{4} \right. \\ \left. Ln \left(\frac{(r_s - r_s \cos(\theta_{EO}) + L_r (1 - \sqrt{1 - (\frac{r_s}{L_r})^2 \sin^2 \theta_{EO}}) + L_{dv})}{(r_s - r_s \cos(\theta_{CC}) + L_r (1 - \sqrt{1 - (\frac{r_s}{L_r})^2 \sin^2 \theta_{CC}}) + L_{dv})} \right) P^{\otimes} [T=T_{expander} \ \& \ \rho=\frac{\dot{m}_c}{V_{min} f}] \right] \quad (25)$$

With constraints :

- As it can be observed on fig. 10, the length of connecting rod should be more than shaft diameter:

$$L_r > 2R_{shaft} \quad (26)$$

- Expander volume at cryogen valve close state should be equal to the cryogen volume entering:

$$\left| \left[(r_s (1 - \cos(\theta_{CC})) + L_r (1 - \sqrt{1 - (\frac{r_s}{L_r})^2 \sin^2 \theta_{CC}}) + L_{dv}) \frac{\pi D_{bore}^2}{4} \right] - \left[\frac{\dot{V}_C^{\otimes} \text{ expander inlet}}{f} \right] \right| < 1e-6 \quad (27)$$

Table 3: Piston expander specifications table

Expander specifications			
Parameter	Variable range	Initial value [14]	Optimized value
Frequency	$30 < f < 100$	50	35.035
Cryogen valve opening degree	$20 < \theta_{CC} < 35$	20	20.0
Bore diameter	$0.01 < D_{bore} < 0.1$	0.06	0.07346
Length of dead volume	$0.001 < L_{dv} < 0.01$	0.002	0.001
Length of connecting rod	$0.05 < L_r < 0.1$	0.1	0.1
Shaft diameter	$0.01 < R_{shaft} < 0.1$	0.02	0.07346
Bore to valve diameter ratio	$3 < ratio_{B/V} < 6$	4	4.1721
Objective function		193.1216	215.4501

- The intake cryogen mass is limited by choking, accordingly it should follow:

$$\dot{m}_c < C_d A \sqrt{\gamma \rho_0 P_0 \left(\frac{2}{\gamma + 1} \right)^{\frac{\gamma+1}{\gamma-1}}} \left(\frac{\theta_{CC}}{360} \right) \quad (28)$$

- Pressure at the inlet should be less than or equal to the maximum pressure allowed within expander, $P_{Mech-limit}$ (Mechanical limit):

$$P_{Mech-limit} > P^@ [T=T_{expander} \ \& \ \rho=\frac{\dot{m}_c}{V_{minf}}] \quad (29)$$

Where $A = \frac{\pi D_{valve}^2}{4}$ and $D_{valve} = \frac{D_{bore}}{ratio_{B/V}}$

It is worth mentioning the initial guess is a scaled version of a design of the piston expander used by Sapin et al.[14] For nitrogen as cryogen the objective function becomes:

$$Obj \ F(Initial \ guess) = -193.1216$$

The optimization is performed using "SciPy" toolbox. The selected method is called "SLSQP" that is best applied for minimizing a scalar function of one or more variables that uses sequential least squares programming. [21] gives:

$$Obj \ F(Initial \ guess) = -215.4501 \quad (30)$$

This indicates importance of expander design to a specific cryogen, due to the fact that each fluid gives certain expansion ratio given the same pressure drop value.

As shown in the fig. 16 and 17 the losses due to expander exhaust decreased from 10.8% in initial design to 5.8% in optimized design.

Table 4: Piston expander optimization effect for 4 selected cryogenes

Expander optimization results				
	Nitrogen	Air	Methane	Hydrogen
Power output initial [W]	3725.87	3698.12	3545.96	4486.83
Power output optimum [W]	4002.33	3972.04	3806.00	4811.03
Entropy generation initial [W/K]	43.4639	43.0027	35.4867	68.1470
Entropy generation Optimum [W/K]	41.3973	41.0270	34.5021	64.9251
2nd law efficiency initial	0.48566	0.48871	0.54161	0.29139
2nd law efficiency optimum	0.51161	0.51364	0.55531	0.32639

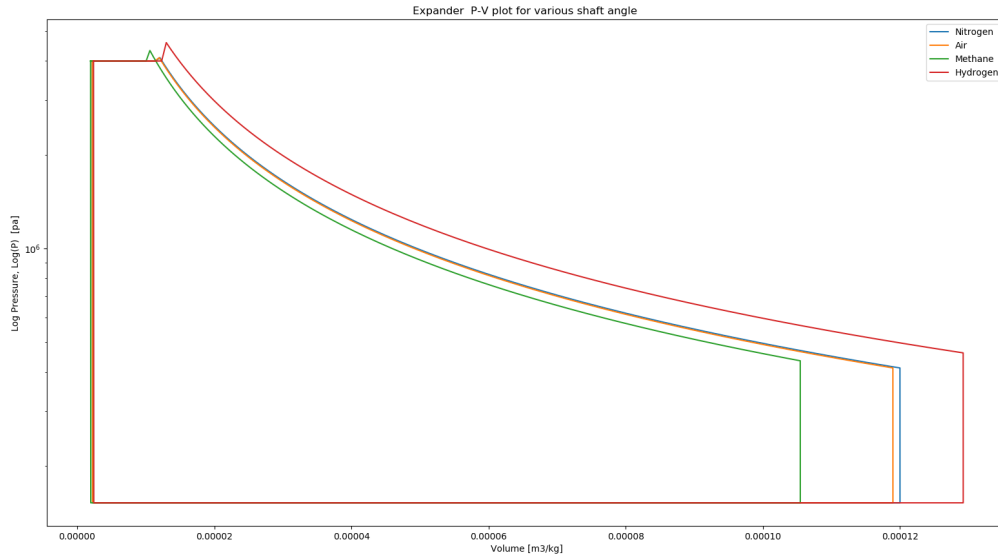


Figure 15: Expander ideal PV plot of specifically optimized design for each cryogenes .

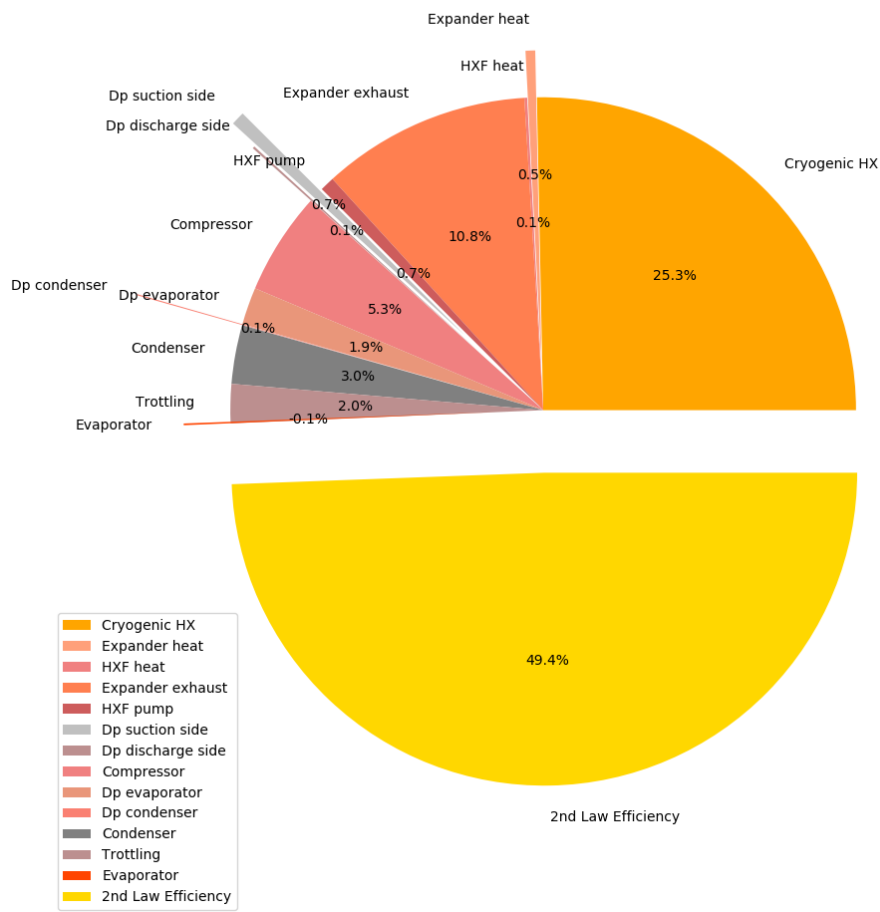


Figure 16: 2nd law efficiency, initial design for nitrogen

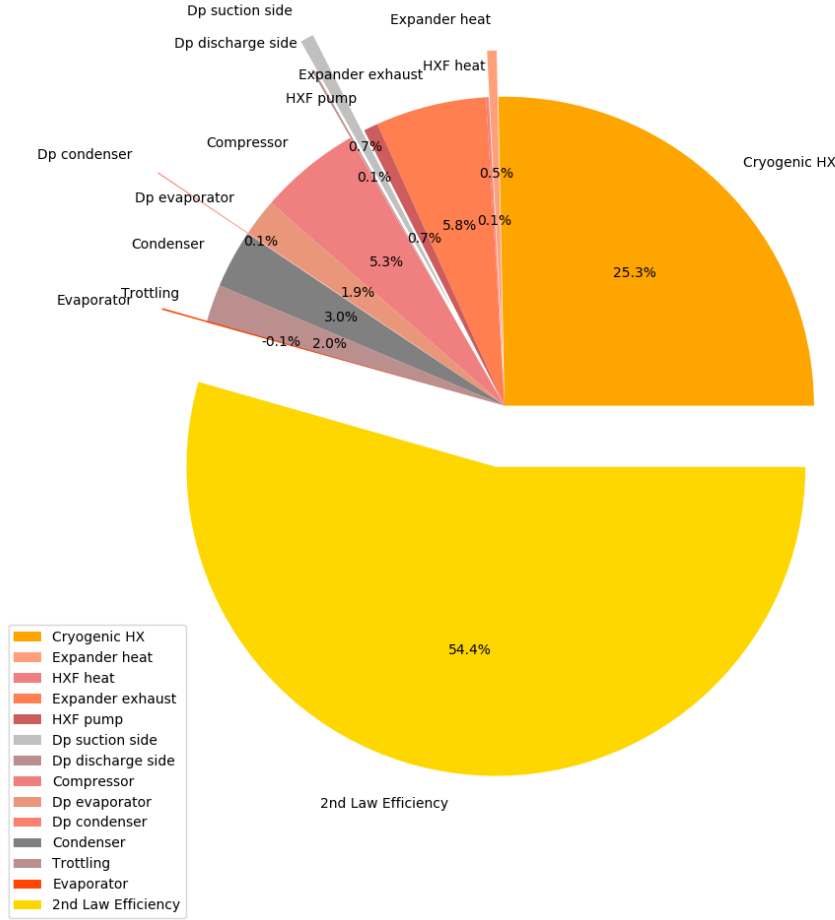


Figure 17: Effect of expander design on 2nd law efficiency; the optimized design for nitrogen

3.3 Improvements on cryogenic heat exchanger(Various cryogen)

The selected fluids considered for comparison are: nitrogen, Air, LNG and hydrogen. The selection of the first 2 is mainly due to ease of production on any location with electricity availability and the 2 latter is due to the potential of getting power-train as well as cooling effect. LNG is already getting widespread as a clean, sustainable and easy to retrofit replacement for diesel. Moreover, for LNG produced from Biogas can bring the emissions to near zero. [27]

Hydrogen on the other hand is considered to be the future of long haul road transportation.[28, 29] Taking a look at the 2nd law analysis, the importance of normal boiling point of each fluid in the CHX losses and as a result on 2nd law efficiency can be seen. Based on equation 18 the heat exchanger loss depend on the normal boiling point of the cryogen since liquid at near ambient is the required condition for storage tank due to the high energy density requiremnet for transport application.

Another way to decrease losses in CHX is to keep the cryogen as saturated liquid at higher pressure and higher temperature, this increases T_{cold}^{in} and as a result decreases the losses in heat exchanger, but there would be a penalty on energy density of the cryogen.

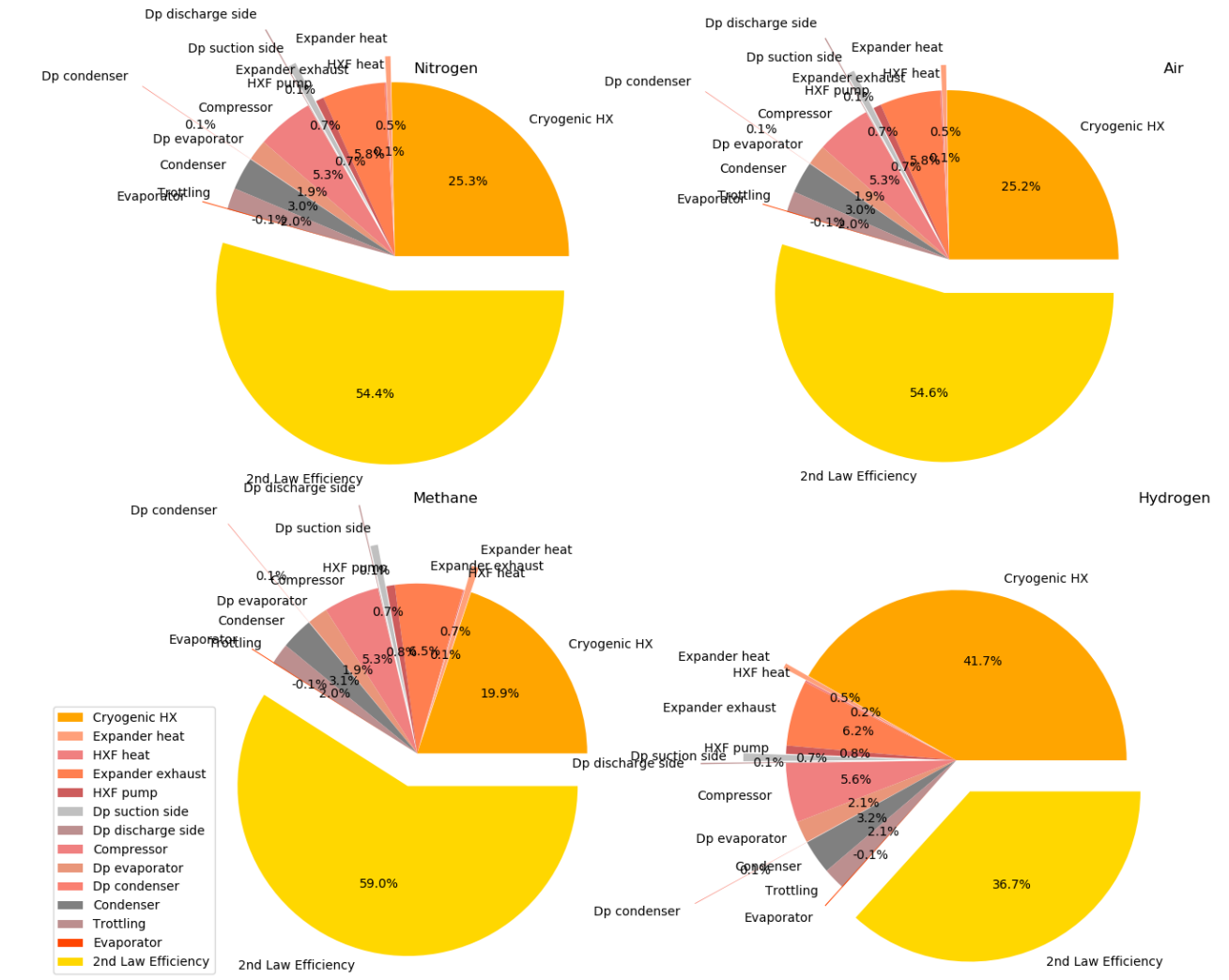


Figure 18: 2nd law analysis of 4 selected cryogenes with optimized design of expander.

3.4 Modifications on vapor compression cycle

3.4.1 Various refrigerant

Most popular refrigerant currently used in transport refrigeration is R404A(GWP=3922), considering the new regulations it will phased out(new installations) by 2020, R22(GWP=1810) has similar condition. Accordingly two natural refrigerants with zero ODP and very low GWP, CO_2 (R744 in subcritical refrigeration cycle) and n-Propane(R290) were chosen for comparison.[30] From the performance point of view, n-Propane provides decent COP as indicated on fig.20, furthermore the low GWP(=3) and zero ODP makes it an ideal refrigerant. Considering the TRU application(outdoor) and with worst case off-design condition, the mass flow rate of refrigerant required(0.035 kg n-Propane) is far below the limits set by European commission on n-Propane usage.[31]

3.4.2 VCC component modifications

The vapor compression refrigeration cycle is compared in various configurations and various complexity level, the current system used in transport refrigeration is single stage VCC with 4 main components.[3] The goal here is to observe system performance improvements in the case of adding further components to improve system performance. In total 6 various cases with their TDN states shown in figure19 were considered and the performance evaluated accordingly as depicted on fig. 20.

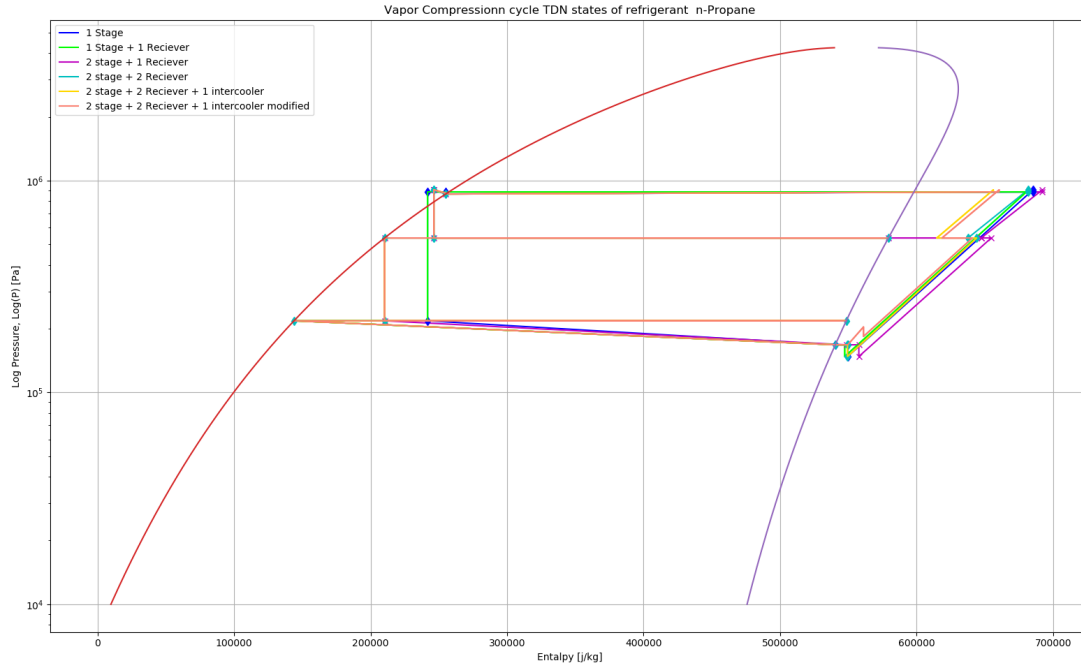


Figure 19: Various configurations of VCC; Propane as the refrigerant

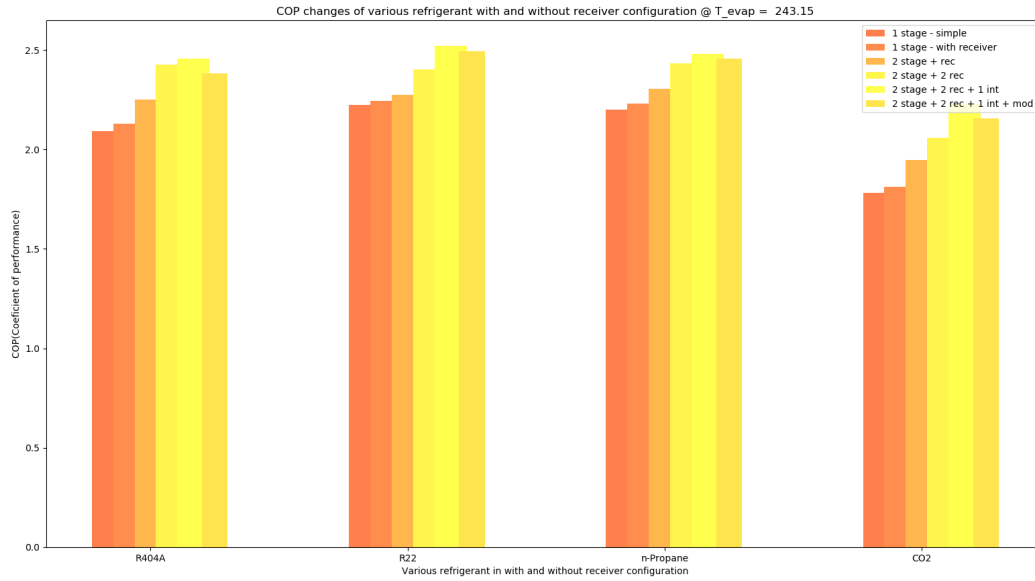


Figure 20: COP values for each configuration of VCC

In general adding components tend to increase the system performance, though the extra complexity and extra cost limits the use of two stage process specially in transport application. The gain in COP by improving the refrigeration cycle is clearly more important at low evaporator temperature as it can be seen from fig. 21 and 22. This suggests the selection of highly efficient system relies heavily on the intended application of the refrigeration unit (Ranging from -20°C for frozen meat to 8°C for fruits or bread). In other words the lower the evaporation temperature the more it viable and economical it will be to use a more complex and efficient system.

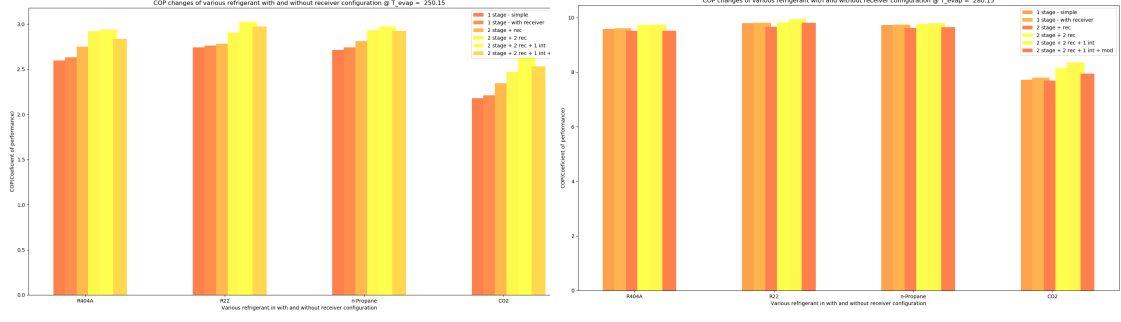


Figure 21: COP variation for various configuration and refrigerants at 250k evaporator temperature

Figure 22: COP variation for various configuration and refrigerants at 280k evaporator temperature

3.5 Two-stage expansion

Due to the mechanical limitations, the pressure difference on piston inlet and outlet cannot exceed 50 bar; though it is possible to break the pressure in two levels (High and low) so to extract more power, similar work was performed by Liu et al. for air expander engine.[18] The compressed air flow is sent to a twin expansion chamber with 2 pistons connected by a connecting rod to a main shaft; the air passing from first chamber expands and then enters the second chamber and after work extraction it is exhausted to the ambient. There is a possibility of using double expander compressor to extract power while directly compressing the refrigerant in the VCC via shaft connected on the other end. The use of double expander compressor has been examined by Heyl. and Quack [32] with application on trans-critical CO_2 refrigeration. With double expander-compressor system, there is the possibility of utilizing higher pressure exergies. As indicated on fig.23 this system is gaining the benefits of having a two stage VCC which as depicted earlier in fig.20; the COP would be higher as well due to inter-cooling after low temperature compressor.

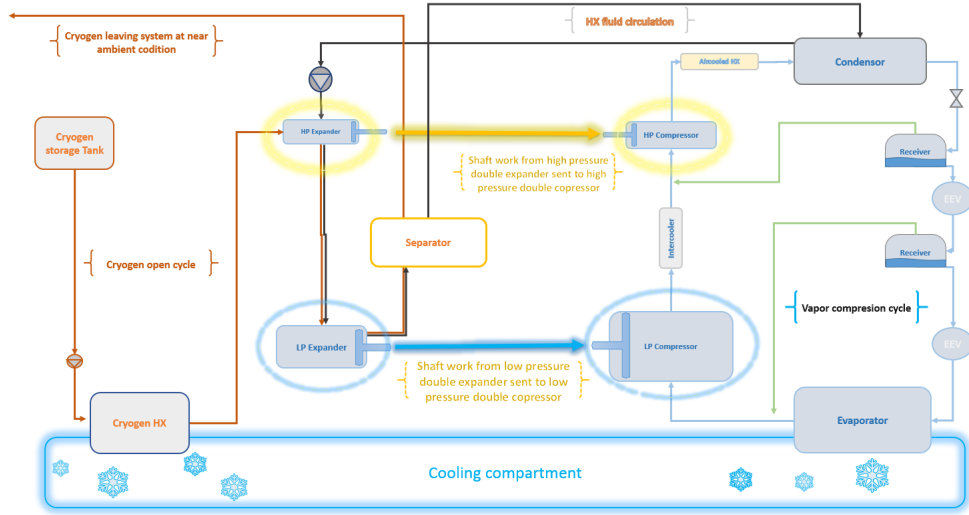


Figure 23: Modified system of two-stage expander, double expander-compressor configuration

The final contribution of each improvements can be seen while comparing the amount of cooling effect produced per kg of cryogen. Table 5 shows the contribution of each modifications for the 4 selected cryogens.

Table 5: Cooling effect in [kWh/kg] of 4 selected cryogenes

Cooling produced in kWh per kg of cryogen in various configuration				
	nitrogen	Air	Methane	hydrogen
Initial condition	649.6	635.1	1231.2	7219.1
Optimized piston expander	697.5	681.4	1317.9	7442.8
Optimized Two-stage inter-cooled VCC	751.2	733.2	1411.4	8588.4
2 stage expansion/ compression	872.8	850.3	1610.7	10323.1

4 Off-design conditions and system performance variations

The system was initially designed for ambient temperature of 20 °C, evaporator temperature of -30 °C and cooling requirement of 15 KW. Based on the application and location these may vary, these 3 different conditions were considered and compared.

4.1 Ambient temperature

Ambient temperature controls the condenser outlet temperature and the expander expansion process temperature; the former rise lead to a drop in COP of VCC while for the latter, this increase translates into slight grow of the work output. The overall effect as indicated in fig. 24 is a drop in cooling production per kg off cryogen as the ambient temperature increases. It should be noted that the frequency should be varied based on the temperature changes to maintain pressure in the optimum condition for any operating condition.

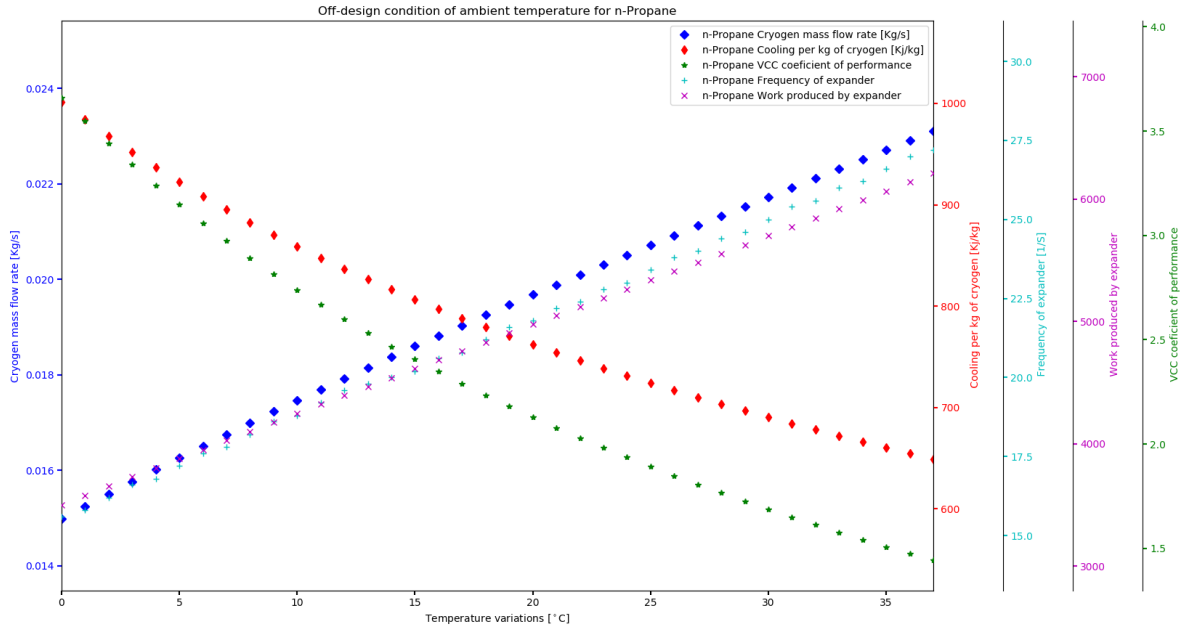


Figure 24: Ambient temperature off-design condition for n-Propane and nitrogen as cryogen.

4.2 Evaporator temperature

Evaporator temperature is specified by the requirements of cargo to be shipped. A range of temperatures are considered from -25°C to 7°C representing various reefer temperature requirements. The variations in cryogen mass flow rate requires adjustment of frequency of piston expander to maintain the optimum pressure values. It is rather intuitive that increasing the evaporator temperature, increases the Carnot efficiency that means the real COP would rise as well.

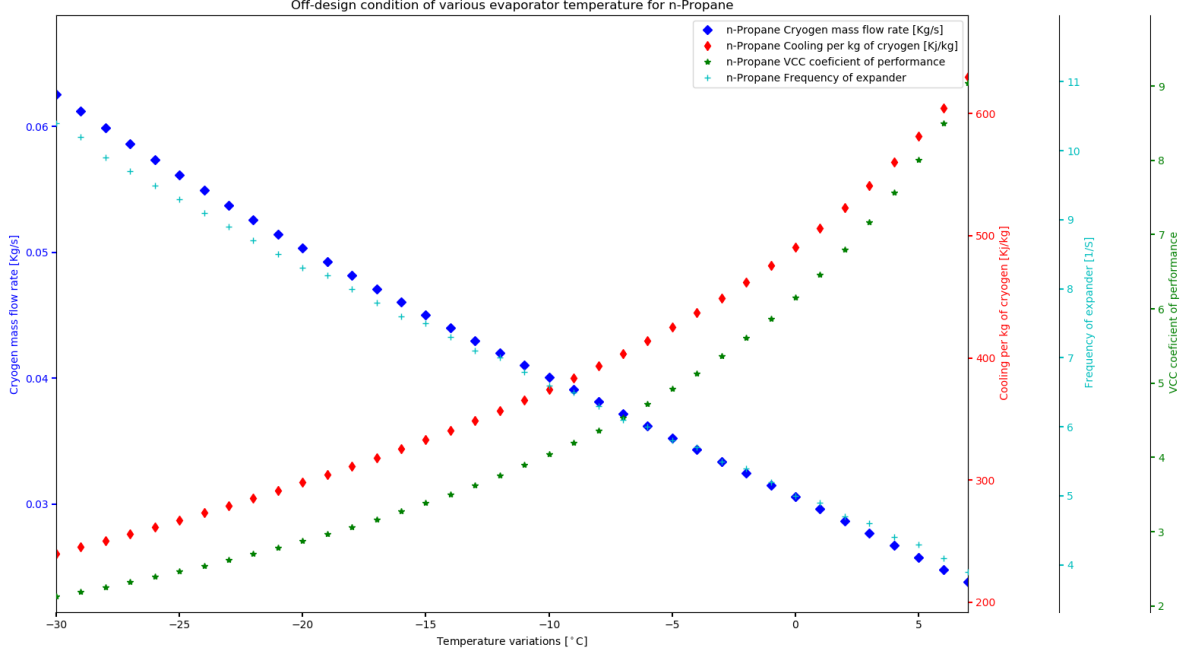


Figure 25: Evaporator temperature off-design condition for n-Propane and nitrogen as cryogen.

4.3 Cooling power required

There are several factors contributing to the cooling power requirement variations, door opening duration, door opening frequency, ambient temperature and quality of the isolating material are among them. Need for extra cooling means more cryogen consumption that translates into the higher rotational speed in the piston expander as well as the compressor connected to it.

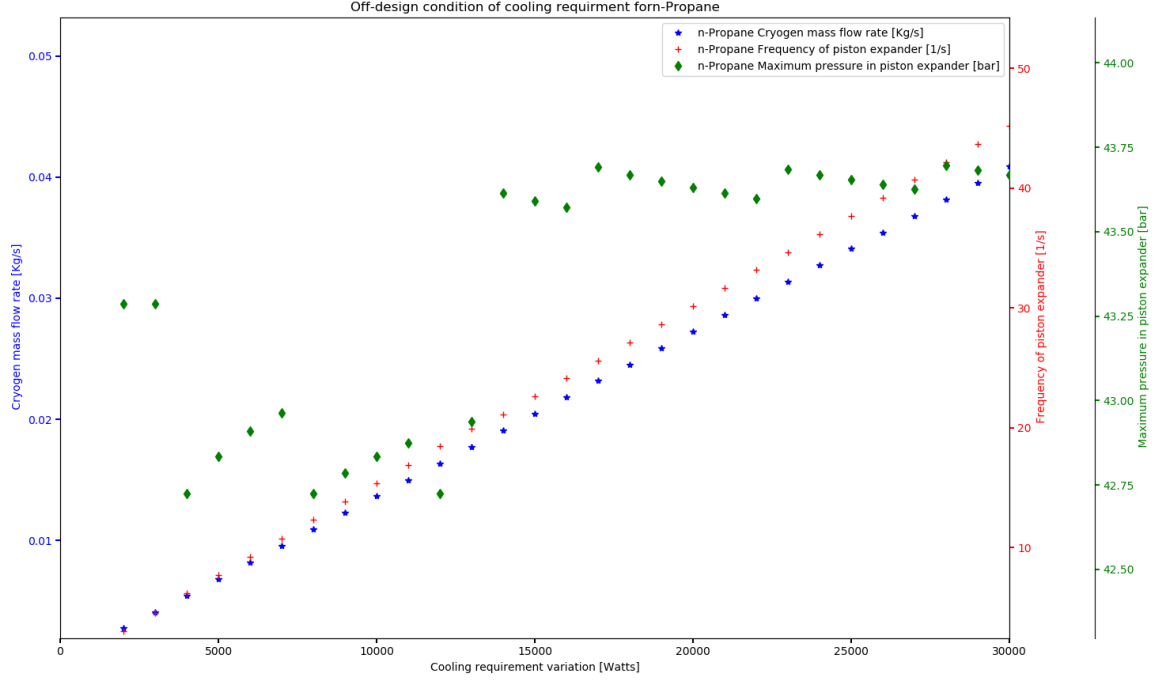


Figure 26: Cooling power requirement off-design condition for n-Propane and nitrogen as cryogen.

5 Conclusion

The inevitable transition toward clean sustainable solutions will affect the transport refrigeration and the role of hydrogen and LNG can be determining as the sources that can provide both cooling and power-train from same fuel, while preventing the cold and pressure exergy from being wasted.

According to the 2nd law analysis of the system, 3 main losses are due to entropy generations in: 1- cryogenic fluid exchanging heat with the cooling compartment 2-Expander losses due to the flow leaving at pressure higher than atmospheric pressure 3-Compressor in vapor compression cycle. Optimization process revolved around the 3 losses improving the overall cryogen consumption by 30-42 % depending on cryogen selected. Accordingly, the piston expander optimization process led to work output increase by 7.4 %, 7.3%, 7% and 3.1% for nitrogen, Air, LNG and hydrogen respectively.

The second law efficiencies after piston expander optimization of the basic system (Single stage expansion and single stage VCC) are: 54.4%, 54.6 %, 59%, 36.7 % for nitrogen, Air, Methane and hydrogen respectively. This suggests the round-trip efficiency of the system using Methane as the cryogen would be the highest of all 4. Cooling based on liquid air or nitrogen is suffering in terms of round-trip efficiency (35%) and low energy density. Furthermore, the requirement of a separate fuel tank different from the one of power-train is a limiting factor adding up to the cost and weight of the overall system. This can still be an economically viable option in case it is combined with LNG regasification plant to produce cheap LiN or LiA.

LNG is a cheap and easy to retrofit alternative for diesel that can decrease CO_2 emissions by 95% if produced from Bio-gas. Considering the average fuel consumption of 1 kg per 5 km for power-train of a 53 ft long truck, the cooling produced only from physical exergy of LNG can be as high as 11 kw cooling. This means the cooling is obtained from same fuel as power-train as a useful byproduct. The LNG "Evaporative + Expander" solution provides cheapest 10 year cost of ownership and lowest emission among the considered scenarios.

Fuel cell (PEM FC) is expensive to run (assuming hydrogen price of 9.5 €/kg) but considering the current trend in the cost of hydrogen production and ease of energy storage using hydrogen from intermittent renewable sources, it can be considered as viable option in near future. The other case that can be considered is, compressed hydrogen "Expander" that emits and costs similar to LNG "Evaporative + Expander", the only limitation is requirement of having the power-train running on hydrogen. Assuming value from Nikola trucks that consumes on average

1kg H₂ per 12 km, the amount of cooling that can be produced is almost 12 kw which is a decent value for a 53ft truck with frequent door open-close condition. In case of using the LiH instead of compressed hydrogen, there will be surplus electricity which can be used to power truck auxiliary or as powertrain, a benefit would be higher volumetric energy density of the fuel($\rho_{H_2}^{-256^{\circ}C \text{ \& } 1bar} = 70.9 \text{ kg/m}^3$ vs. $\rho_{H_2}^{25^{\circ}C \text{ \& } 700bar} = 39.1 \text{ kg/m}^3$) but leading to a higher cost of production.

Overall, the use cryogenic fluid expansion and thermal exergy is a sustainable and cost effective method for transport refrigeration and LNG and hydrogen can play key role in that regards.

References

- [1] Bejan, A. *Advanced Engineering Thermodynamics*. John Wiley & Sons, New York, 1997.
- [2] Liquid air electricity storage facility, Highwire, by Baker Hughs, A GE company, **High-view power**
- [3] Liquid Air on the European Highway, The economic and environmental impact of zero-emission transport refrigeration **Dearman**, 2015
- [4] Karakas A, Egrican N, Uygur S. *Second-law analysis of solar absorption cooling cycles using LiBr/water and ammonia/water as working fluids..* Applied Energy Journal 1990;37:169–88.
- [5] D. Richardson *An object oriented simulation framework for steady-state analysis of vapor compression refrigeration systems and components* PhD thesis, Department of Mechanical Engineering, University of Maryland, College Park, 2006
- [6] Bell, Ian H. and Wronski, Jorrit and Quoilin, Sylvain and Lemort, Vincent *Pure and Pseudo-pure Fluid Thermophysical Property Evaluation and the Open-Source Thermophysical Property Library CoolProp* Industrial & Engineering Chemistry Research 53, 6, pages 2498-2508, 2014,doi:10.1021/ie4033999
- [7] N. A. Cumpsty Thermodynamics and Propulsion, MIT, 2003 *Jet Propulsion: A Simple Guide to the Aerodynamic and Thermodynamic Design and Performance of Jet Engines* Cambridge University Press, 14 Aug 2003 - Technology & Engineering
- [8] Robert H. Perry, Don W. Green *Perry's Chemical Engineers handbook*. ISBN 10: 0070498415 ISBN 13: 9780070498419 Edition: 7 Language: english Pages: 2582 McGraw-Hill, 1999.
- [9] Lyle Albright *Albright's Chemical Engineering Handbook 1st Edition*. ISBN-13: 978-0824753627 ISBN-10: 9780824753627 Edition:1 Language: english pages:1909 CRC Press; 1 edition (November 20, 2008)
- [10] Bossel U *Does a hydrogen economy make sense?*. Proc IEEE 2006;94(10):1826–37.
- [11] Quack H. *Conceptual design of a high efficiency large capacity hydrogen liquefier*. Advanced Cryogen Eng 2001;47:255–63.
- [12] Valenti G, Macchi E. *Liquid hydrogen: from clean coal to filling station. Part A: proposal of an innovative, highly-efficient, large-scale liquefier..* HYSYDAYS—2nd world congress of young scientists on hydrogen energy systems 2007, 2007.
- [13] Valenti G, Macchi E. *Liquid hydrogen: from clean coal to filling station. Part B: analysis of an advanced, highlyintegrated, IGCC-liquefier infrastructure..* HYSYDAYS—2nd world congress of young scientists on hydrogen energy systems 2007, 2007.
- [14] Sapin P.,Taleb A., Barfuss C., White A.J, Fabris D. and Markides C.N *Thermodynamic Losses in a Gas Spring: Comparison of Experimental and Numerical Results*. 12th International Conference on Heat Transfer, Fluid Mechanics and Thermodynamics .
- [15] Simpson M., Rotolo G., Sapin P., De Palma P., White A.J. and Markides C.N *Thermodynamic performance maps of reciprocating-piston expanders for operation at off-design and part-load conditions*. 13th International Conference on Heat Transfer, Fluid Mechanics and Thermodynamics .

- [16] Xiaochen Hou, Hongguang Zhang, Fei Yu, Hongda Liu, Fubin Yang, Xu Yonghong, Yaming Tian, Gaosheng Li *Free piston expander-linear generator used for organic Rankine cycle waste heat recovery system*. Applied Energy, DOI: 10.1016/j.apenergy.2017.09.024.
- [17] Rongliang Zhoua, Tiejun Zhangb, Juan Catanob, John T. Wena,b, Gregory J. Michnac, Yoav Pelesb, Michael K. Jensen *The steady-state modeling and optimization of a refrigeration system for high heat flux removal..* Applied Thermal Engineering 30 (2010) 2347e2356.
- [18] Chi-Min Liu, Chin-Lun Huang, Cheng-Kuo Sung, Chih-Yung Huang *Performance analysis of a two-stage expansion air engine..* Energy 115 (2016) 140e148.
- [19] Gianluca Valenti, Ennio Macchi *Proposal of an innovative, high-efficiency, large-scale hydrogen liquefier*. INTERNATIONAL JOURNAL OF hydrogen ENERGY 33 (2008) 3116 – 3121.
- [20] Leducq, D., Guilpart, J., Trystram, G. *Low order dynamic model of a vapor compression cycle for process control design..* Journal of Food Process Engineering 26 (2003) 67-91.
- [21] Eric Jones and Travis Oliphant and Pearu Peterson and others *SciPy Open source scientific tools for Python*. <http://www.scipy.org/>
- [22] John D. Hunter *Matplotlib: A 2D Graphics Environment..* journal.
- [23] Ireneusz Szczygieł, Wojciech Stanek, Jan Szargut *Application of the Stirling engine driven with cryogenic exergy of LNG(liquefied natural gas) for the production of electricity*. Energy 105 (2016) 25e31
- [24] M. RomeroGómez, R.FerreiroGarcia , J.RomeroGómez , J.CarbiaCarril *Review of thermal cycles exploiting the exergy of liquefied natural gas in the regasification process*. Renewable and Sustainable Energy Reviews 38(2014)781–795
- [25] Kamiyama Naohisa *Air-Conditioning system for LNG automobile..* JP2010105586.
- [26] Paweł Dorosz, Paweł Wojcieszak and Ziemowit Malecha *Exergetic Analysis, Optimization and Comparison of LNG Cold Exergy Recovery Systems for Transportation..* Entropy open access Volume 20, Issue 1. <https://doi.org/10.3390/e20010059>
- [27] Jose Luis Osorio-Tejada , Eva Llera-Sastresa , Sabina Scarpellini *A multi-criteria sustainability assessment for bio-diesel and liquefied natural gas as alternative fuels in transport systems..* Journal of Natural Gas Science and Engineering.
- [28] Cezary Misiópecki *Investigation of fuel cell technology for long-haul trucks..* A Master ´s thesis, The School for Renewable Energy Science.
- [29] Sunita Sharma , Sib Krishna Ghoshal *hydrogen the future transportation fuel: From production to applications..* Renewable and Sustainable Energy Reviews.
- [30] *Refrigerants properties*. Linde AG, Gases Division, Seitnerstrasse 70, 82049 Pullach, Germany
- [31] authors *National Codes, Standards and Legislation of EU Member States with respect to F-Gas alternatives*. Report for European Commission, DG Clima
- [32] P. Heyl, H. Quack *Free piston expander-compressor for CO₂ design application and results..* TU Dresden, Germany..
- [33] Lin Gao *Well-to-Wheels Analysis of Energy Use and Greenhouse Gas Emissions for Alternative Fuels..* International Journal of Applied Science and Technology .
- [34] Norman Brinkman, Michael Wang, Trudy Weber, Thomas Darlington *Well-to-Wheels Analysis of Advanced Fuel/Vehicle Systems — A North American Study of Energy Use, Greenhouse Gas Emissions, and Criteria Pollutant Emissions* . Department of Energy report, May 2005
- [35] Angela Mutumba, Kevin Cheeseman, Henry Clarke, Dongsheng Wen *Design and development of a direct injection system for cryogenic engines*. Cryogenics 91 (2018) 77–86.

- [36] Inkyu Lee , Jinwoo Park , Fengqi You , Il Moon *A novel cryogenic energy storage system with LNG direct expansion regasification: Design, energy optimization, and exergy analysis*. Energy 173 (2019) 691e705
- [37] Ole Kolb, Stefan Siegemund *Study on the Implementation of Article 7(3) of the “Directive on the Deployment of Alternative Fuels Infrastructure” – Fuel Price Comparison*. Directorate-General for Mobility and Transport, Directorate B Investment, Innovative & Sustainable, Unit B4 Sustainable & Intelligent Transport - January – 2017
- [38] Yajun Li, Fangfang Bai *Integrated and Cost-effective Design Utilizes LNG Cryogenic Energy for Power Generation*. 978-1-4244-2487-0/09/\$25.00 ©2009 IEEE.
- [39] Jia Wang , Weiqing Xu , Shuiting Ding , Yan Shi , Maolin Cai , Ali Rehman *Liquid air fueled open-closed cycle Stirling engine and its exergy analysis*. Energy 90 (2015) 187e201.
- [40] Tianbiao He, Zheng Rong Chong , Junjie Zheng , Yonglin Ju , Praveen Linga *LNG cold energy utilization: Prospects and challenges*. Energy 170 (2019) 557e568.
- [41] Nikola Motor Company. *Website*.(<http://nikolamotor.com/motor>). [Accessed September 2019].

TDN points	Pressure (pa)	Enthalpy (kJ/kg)	Temperature (K)	Entropy (kJ/kg/K)	Volume (M3/kg)	Phase/Quality	Fluid	Mass flow rate (kg/s)
0	884508.5662	246.334	291.15	1.16141	0.00199	Sat Liq	'n-Propane'	0.029567275
1	536170.3612	246.334	277.21765	1.16699	0.01012	0.09781	'n-Propane'	0.029567275
2	536170.36	579.31713	277.21765	2.36815	0.08582	Sat Vap	'n-Propane'	0.029567275
3	536170.36	210.2358	277.21765	1.03677	0.00191	0	'n-Propane'	0.029567275
4	237832.16	210.2358	252.38236	1.05009	0.0297	0.15108	'n-Propane'	0.029567275
5	237832.16	551.23726	252.38236	2.40122	0.18647	Sat Liq	'n-Propane'	0.029567275
6	237832.16	149.54715	252.38236	0.80962	0.0018	0	'n-Propane'	0.029567275
7	167832.16	540.38392	243.15	2.41917	0.25861	Sat Liq	'n-Propane'	0.029567275
8	167832.16	547.98338	248.15	2.4501	0.26492	Gas	'n-Propane'	0.029567275
9	178407.98	548.47499	248.79726	2.44115	0.24912	Gas	'n-Propane'	0.029567275
10	158407.98	548.47499	248.18207	2.46246	0.28159	Gas	'n-Propane'	0.029567275
11	536170.36	637.22984	309.40141	2.56573	0.10002	Gas	'n-Propane'	0.029567275
12	536170.36	618.55928	299.15	2.50437	0.09564	Gas	'n-Propane'	0.029567275
13	536170.36	614.72118	297.02524	2.49149	0.09472	Gas	'n-Propane'	0.029567275
14	904508.57	656.15757	325.16581	2.5366	0.05963	Gas	'n-Propane'	0.029567275
15	884508.57	656.15757	324.86361	2.54032	0.0611	Gas	'n-Propane'	0.029567275
16	864508.57	257.35958	294.40748	1.19916	0.00236	0.0069	'n-Propane'	0.029567275
0	202650	-121.94806	77.35483	2.83346	0.00124	Liq	'Nitrogen'	0.017038158
1	10000000	220.87161	243.15	5.15343	0.00685	Gas	'Nitrogen'	0.017038158
2	10000000	283.71388	293.15	5.38882	0.00871	Gas	'Nitrogen'	0.017038158
3	3999999.42	295.3633	293.15	5.69928	0.02163	Gas	'Nitrogen'	0.017038158
4	214949.703	303.79677	293.15	6.59365	0.40458	Gas	'Nitrogen'	0.017038158
5	101325	304.06023	293.15	6.81768	0.85849	Gas	'Nitrogen'	0.017038158
0	101325	0	293.15	0	0.00093	Liq	Ethylene Glycol 60% Volume	0.309744412
1	101325	40.86038	306.17106	0.13636	0.00094	Liq	Ethylene Glycol 60% Volume	0.309744412
2	101325	18.69941	299.15	0.06314	0.00093	Liq	Ethylene Glycol 60% Volume	0.309744412
3	4000000	21.71313	299.15	0.06108	0.00093	Liq	Ethylene Glycol 60% Volume	0.309744412
4	4000000	3.04362	293.15	-0.00196	0.00093	Liq	Ethylene Glycol 60% Volume	0.309744412
5	4000000	3.04362	293.15	-0.00196	0.00093	Liq	Ethylene Glycol 60% Volume	0.309744412

Figure 27: Thermodynamic states and properties of n-Propane as refrigerant, nitrogen as cryogen and Ethylene Glycol 60% as HXF

TDN points	Pressure (pa)	Enthalpy (kJ/kg)	Temperature (K)	Entropy (kJ/kg/K)	Volume (M3/kg)	Phase/Quality	Fluid	Mass flow rate (kg/s)
0	884508.5662	246.334	291.15	1.16141	0.00199	Sat Liq	'n-Propane'	0.029283387
1	536170.3612	246.334	277.21765	1.16699	0.01012	0.09781	'n-Propane'	0.029283387
2	536170.3612	579.31713	277.21765	2.36815	0.08582	Sat Vap	'n-Propane'	0.029283387
3	536170.3612	210.2358	277.21765	1.03677	0.00191	0	'n-Propane'	0.029283387
4	237832.1561	210.2358	252.38236	1.05009	0.0297	0.15108	'n-Propane'	0.029283387
5	237832.1561	551.23726	252.38236	2.40122	0.18647	Sat Liq	'n-Propane'	0.029283387
6	237832.1561	149.54715	252.38236	0.80962	0.0018	0	'n-Propane'	0.029283387
7	167832.1561	540.38392	243.15	2.41917	0.25861	Sat Liq	'n-Propane'	0.029283387
8	167832.1561	547.98338	248.15	2.4501	0.26492	Gas	'n-Propane'	0.029283387
9	178407.9833	548.47499	248.79726	2.44115	0.24912	Gas	'n-Propane'	0.029283387
10	158407.9833	548.47499	248.18207	2.46246	0.28159	Gas	'n-Propane'	0.029283387
11	536170.3612	637.22984	309.40141	2.56573	0.10002	Gas	'n-Propane'	0.029283387
12	536170.3612	618.55928	299.15	2.50437	0.09564	Gas	'n-Propane'	0.029283387
13	536170.3612	614.72118	297.02524	2.49149	0.09472	Gas	'n-Propane'	0.029283387
14	904508.5662	656.15757	325.16581	2.5366	0.05963	Gas	'n-Propane'	0.029283387
15	884508.5662	656.15757	324.86361	2.54032	0.0611	Gas	'n-Propane'	0.029283387
16	864508.5662	257.35958	294.40748	1.19916	0.00236	0.0069	'n-Propane'	0.029283387
0	202650	0.06758	78.90278	-0.00061	0.00114	Liq	'Air'	0.017521007
1	10000000	336.82277	243.15	2.2494	0.00649	Gas	'Air'	0.017521007
2	10000000	398.19853	293.15	2.47987	0.00832	Gas	'Air'	0.017521007
3	4000000	410.47852	293.15	2.78147	0.02081	Gas	'Air'	0.017521007
4	214949.745	419.1352	293.15	3.64679	0.39117	Gas	'Air'	0.017521007
5	101325	419.40492	293.15	3.86347	0.83017	Gas	'Air'	0.017521007
0	101325	0	293.15	0	0.00093	Liq	Ethylene Glycol 60% Volume	0.306993473
1	101325	40.83069	306.16172	0.13627	0.00094	Liq	Ethylene Glycol 60% Volume	0.306993473
2	101325	18.69941	299.15	0.06314	0.00093	Liq	Ethylene Glycol 60% Volume	0.306993473
3	4000000	21.71313	299.15	0.06108	0.00093	Liq	Ethylene Glycol 60% Volume	0.306993473
4	4000000	3.04362	293.15	-0.00196	0.00093	Liq	Ethylene Glycol 60% Volume	0.306993473
5	4000000	3.04362	293.15	-0.00196	0.00093	Liq	Ethylene Glycol 60% Volume	0.306993473

Figure 28: Thermodynamic states and properties of n-Propane as refrigerant, Air as cryogen and Ethylene Glycol 60% as HXF

TDN points	Pressure (pa)	Enthalpy (kJ/kg)	Temperature (K)	Entropy (kJ/kg/K)	Volume (M3/kg)	Phase/Quality	Fluid	Mass flow rate (kg/s)
0	884508.5662	246.334	291.15	1.16141	0.00199	Sat Liq	'n-Propane'	0.026921867
1	536170.3612	246.334	277.21765	1.16699	0.01012	0.09781	'n-Propane'	0.026921867
2	536170.3612	579.31713	277.21765	2.36815	0.08582	Sat Vap	'n-Propane'	0.026921867
3	536170.3612	210.2358	277.21765	1.03677	0.00191	0	'n-Propane'	0.026921867
4	237832.1561	210.2358	252.38236	1.05009	0.0297	0.15108	'n-Propane'	0.026921867
5	237832.1561	551.23726	252.38236	2.40122	0.18647	Sat Liq	'n-Propane'	0.026921867
6	237832.1561	149.54715	252.38236	0.80962	0.0018	0	'n-Propane'	0.026921867
7	167832.1561	540.38392	243.15	2.41917	0.25861	Sat Liq	'n-Propane'	0.026921867
8	167832.1561	547.98338	248.15	2.4501	0.26492	Gas	'n-Propane'	0.026921867
9	178407.9833	548.47499	248.79726	2.44115	0.24912	Gas	'n-Propane'	0.026921867
10	158407.9833	548.47499	248.18207	2.46246	0.28159	Gas	'n-Propane'	0.026921867
11	536170.3612	637.22984	309.40141	2.56573	0.10002	Gas	'n-Propane'	0.026921867
12	536170.3612	618.55928	299.15	2.50437	0.09564	Gas	'n-Propane'	0.026921867
13	536170.3612	614.72118	297.02524	2.49149	0.09472	Gas	'n-Propane'	0.026921867
14	904508.5662	656.15757	325.16581	2.5366	0.05963	Gas	'n-Propane'	0.026921867
15	884508.5662	656.15757	324.86361	2.54032	0.0611	Gas	'n-Propane'	0.026921867
16	864508.5662	257.35958	294.40748	1.19916	0.00236	0.0069	'n-Propane'	0.026921867
0	202650.00	0.14608	111.66697	-0.00084	0.00237	Liq	'Methane'	0.009509736
1	10000000.00	614.50339	243.15	3.31341	0.00815	Gas	'Methane'	0.009509736
2	10000000.00	794.32195	293.15	3.99016	0.01277	Gas	'Methane'	0.009509736
3	3999999.57	858.45021	293.15	4.63077	0.03527	Gas	'Methane'	0.009509736
4	214949.71	897.6774	293.15	6.24422	0.70403	Gas	'Methane'	0.009509736
5	101325.00	898.82204	293.15	6.63682	1.49665	Gas	'Methane'	0.009509736
0	101325.00	0	293.15	0	0.00093	Liq	Ethylene Glycol 60% Volume	0.297972068
1	101325.00	38.67445	305.48265	0.12922	0.00093	Liq	Ethylene Glycol 60% Volume	0.297972068
2	101325.00	18.69941	299.15	0.06314	0.00093	Liq	Ethylene Glycol 60% Volume	0.297972068
3	4000000.00	21.71313	299.15	0.06108	0.00093	Liq	Ethylene Glycol 60% Volume	0.297972068
4	4000000.00	3.04362	293.15	-0.00196	0.00093	Liq	Ethylene Glycol 60% Volume	0.297972068
5	4000000.00	3.04362	293.15	-0.00196	0.00093	Liq	Ethylene Glycol 60% Volume	0.297972068

Figure 29: Thermodynamic states and properties of n-Propane as refrigerant, Methane as cryogen and Ethylene Glycol 60% as HXF

TDN points	Pressure (pa)	Enthalpy (kJ/kg)	Temperature (K)	Entropy (kJ/kg/K)	Volume (M3/kg)	Phase/Quality	Fluid	Mass flow rate (kg/s)
0	884508.5662	246.334	291.15	1.16141	0.00199	Sat Liq	'n-Propane'	0.035105596
1	536170.3612	246.334	277.21765	1.16699	0.01012	0.09781	'n-Propane'	0.035105596
2	536170.3612	579.31713	277.21765	2.36815	0.08582	Sat Vap	'n-Propane'	0.035105596
3	536170.3612	210.2358	277.21765	1.03677	0.00191	0	'n-Propane'	0.035105596
4	237832.1561	210.2358	252.38236	1.05009	0.0297	0.15108	'n-Propane'	0.035105596
5	237832.1561	551.23726	252.38236	2.40122	0.18647	Sat Liq	'n-Propane'	0.035105596
6	237832.1561	149.54715	252.38236	0.80962	0.0018	0	'n-Propane'	0.035105596
7	167832.1561	540.38392	243.15	2.41917	0.25861	Sat Liq	'n-Propane'	0.035105596
8	167832.1561	547.98338	248.15	2.4501	0.26492	Gas	'n-Propane'	0.035105596
9	178407.9833	548.47499	248.79726	2.44115	0.24912	Gas	'n-Propane'	0.035105596
10	158407.9833	548.47499	248.18207	2.46246	0.28159	Gas	'n-Propane'	0.035105596
11	536170.3612	637.22984	309.40141	2.56573	0.10002	Gas	'n-Propane'	0.035105596
12	536170.3612	618.55928	299.15	2.50437	0.09564	Gas	'n-Propane'	0.035105596
13	536170.3612	614.72118	297.02524	2.49149	0.09472	Gas	'n-Propane'	0.035105596
14	904508.5662	656.15757	325.16581	2.5366	0.05963	Gas	'n-Propane'	0.035105596
15	884508.5662	656.15757	324.86361	2.54032	0.0611	Gas	'n-Propane'	0.035105596
16	864508.5662	257.35958	294.40748	1.19916	0.00236	0.0069	'n-Propane'	0.035105596
0	202650	0.94591	20.36884	-0.02371	0.01409	Liq	'Hydrogen'	0.001420746
1	10000000	3182.42116	243.15	31.39972	0.10714	Gas	'Hydrogen'	0.001420746
2	10000000	3905.62802	293.15	34.10411	0.12826	Gas	'Hydrogen'	0.001420746
3	3999999.997	3877.09188	293.15	37.93524	0.3095	Gas	'Hydrogen'	0.001420746
4	214953.883	3860.79301	293.15	50.03103	5.63206	Gas	'Hydrogen'	0.001420746
5	101325	3860.32199	293.15	53.13419	11.93999	Gas	'Hydrogen'	0.001420746
0	101325	0	293.15	0	0.00093	Liq	Ethylene Glycol 60% Volume	0.361990772
1	101325	41.51198	306.3761	0.13849	0.00094	Liq	Ethylene Glycol 60% Volume	0.361990772
2	101325	18.69941	299.15	0.06314	0.00093	Liq	Ethylene Glycol 60% Volume	0.361990772
3	4000000	21.71313	299.15	0.06108	0.00093	Liq	Ethylene Glycol 60% Volume	0.361990772
4	4000000	3.04362	293.15	-0.00196	0.00093	Liq	Ethylene Glycol 60% Volume	0.361990772
5	4000000	3.04362	293.15	-0.00196	0.00093	Liq	Ethylene Glycol 60% Volume	0.361990772

Figure 30: Thermodynamic states and properties of n-Propane as refrigerant, hydrogen as cryogen and Ethylene Glycol 60% as HXF